Published in final edited form as:

J Comp Neurol. 2020 February 01; 528(2): 283–307. doi:10.1002/cne.24753.

Dual recombinase fate mapping reveals a transient cholinergic phenotype in multiple populations of developing glutamatergic neurons

Nailyam Nasirova[1], **Lely A. Quina**[1], **Ibis M. Agosto-Marlin**[1], **Jan-Marino Ramirez**[1], **Evelyn K. Lambe**[3], **Eric E. Turner**[1,2,4]

[1]Center for Integrative Brain Research, Seattle Children's Research Institute

[2]Department of Psychiatry and Behavioral Sciences, University of Washington, Seattle WA, 98101

[3]Departments of Physiology, Obstetrics and Gynecology, and Psychiatry, University of Toronto, Toronto, Ontario M5S 1A8, Canada

Abstract

Cholinergic transmission shapes the maturation of glutamatergic circuits, yet the developmental sources of acetylcholine have not been systematically explored. Here we have used Cre-recombinase mediated genetic labeling to identify and map both mature and developing CNS neurons that express choline acetyltransferase (ChAT). Correction of a significant problem with a widely used Chat^{Cre} transgenic line ensures that this map does not contain expression artifacts. Chat^{Cre} marks all known cholinergic systems in the adult brain, but also identifies several brain areas not usually regarded as cholinergic, including specific thalamic and hypothalamic neurons, the subiculum, the lateral parabrachial nucleus, the cuneate/gracilis nuclei, and the pontocerebellar system. This Chat^{Cre} fate map suggests transient developmental expression of a cholinergic phenotype in areas important for cognition, motor control, and respiration. We therefore examined expression of ChAT and the vesicular acetylcholine transporter (VAChT) in the embryonic and early postnatal brain to determine the developmental timing of this transient cholinergic phenotype, and found that it mirrored the establishment of relevant glutamatergic projection pathways. We then used an intersectional genetic strategy combining Chat^{Cre} with Vglut2^{Flp} to show that these neurons adopt a glutamatergic fate in the adult brain. The transient cholinergic phenotype of these glutamatergic neurons suggests a homosynaptic source of acetylcholine for the maturation of developing glutamatergic synapses. These findings thus define critical windows during which specific glutamatergic circuits may be vulnerable to disruption by nicotine *in utero*, and suggest new mechanisms for pediatric disorders associated with maternal smoking, such as sudden infant death syndrome.

Graphical Abstract

[4]Address for correspondence: Seattle Children's Research Institute, 1900 Ninth Avenue, mail stop C9S-10, Seattle, WA 98101. eric.turner@seattlechildrens.org.

Data availability statement

The data that support the findings of this study are available from the corresponding author upon reasonable request.

A recently emerging theme in neurotransmission is the expression of multiple classical neurotransmitters by many kinds of neurons. Here we have used Cre-recombinase mediated transgenic fate mapping in mice to label all neurons that express, or have a history of expressing, choline acetyltransferase (ChAT) with the fluorescent marker tdTomato. An intersectional Cre/Flp dual recombinase was then used to identify neurons that co-expressed Chat and the subcortical glutamatergic marker, VGluT2. Only a few brain areas, such as the ventral medial habenula, express high levels of both markers in the adult brain. However, this analysis revealed several unsuspected brain regions that express ChAT together with VgluT2 in the developing brain, but are glutamatergic in the adulthood. These findings have significant implications for the role of acetylcholine in the maturation of excitatory circuits.

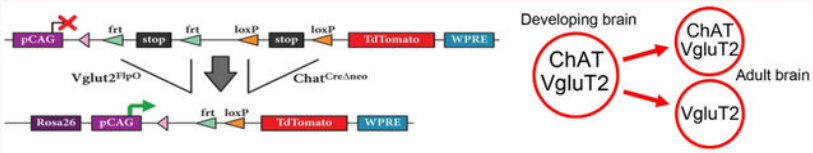

Keywords

choline acetyltransferase; acetylcholine; glutamate; RRID: AB_2079751; RRID: AB_2209751; RRID: AB_2068524; RRID: AB_2064130; RRID: AB_2576200

INTRODUCTION

Acetylcholine (ACh) is used as a neurotransmitter by several well-characterized systems in the adult brain, including the striatum, the septum/diagonal band, the ascending forebrain cholinergic system, cholinergic neurons of the mesopontine tegmentum, and motor neurons throughout the brainstem and spinal cord (Woolf, 1991). Although ACh is the sole fast neurotransmitter in motor neurons, in the central nervous system it is becoming increasingly clear that ACh may act in concert with other co-expressed fast neurotransmitters. Striatal cholinergic neurons can exhibit glutamatergic transmission dependent on the glutamate transporter VGluT3 (Boulland et al., 2004; Gras et al., 2002; Higley et al., 2011), which is atypical in that it is generally co-expressed in neurons with other neurotransmitters (El Mestikawy, Wallen-Mackenzie, Fortin, Descarries, & Trudeau, 2011). GABA has also been identified as a co-transmitter in cholinergic neurons (Granger, Mulder, Saunders, & Sabatini, 2016; Saunders, Granger, & Sabatini, 2015; Takacs et al., 2018). Broadly, these findings fit into the increasing recognition of the cellular co-expression of classical neurotransmitters, particularly GABA or glutamate together with monoamines, that has emerged in several brain systems (Granger, Wallace, & Sabatini, 2017; Hnasko & Edwards, 2012; Trudeau et al., 2014).

Neurons in the ventral medial habenula (MHbV) have also been identified as cholinergic (Contestabile et al., 1987; Kataoka, Nakamura, & Hassler, 1973). However, these neurons co-express the principal subcortical glutamate transporter VGluT2 (Qin & Luo, 2009), and optogenetic experiments have shown that fast synaptic transmission from MHbV neurons to their postsynaptic targets in the interpeduncular nucleus (IP) is mediated primarily by

glutamate (Hsu et al., 2013; Ren et al., 2011). Specific loss of ChAT activity in the MHb results in a reduction of glutamatergic transmission at the MHbV-IP synapse (Frahm et al., 2015). Neurons that co-express ChAT and VGluT2 also include the so-called postinspiratory complex (PiCo), a group of medullary neurons critically involved in respiratory rhythmogenesis (T. M. Anderson et al., 2016). The rhythmic activity in this area depends on glutamatergic signaling, while ACh, as in the MHbV, appears to serve a modulatory role. Use of both ACh and glutamate has also been identified in the recurrent projections of neonatal spinal motor neurons (Mentis et al., 2005; Nishimaru, Restrepo, Ryge, Yanagawa, & Kiehn, 2005).

These diverse examples call for a systematic examination of the full extent of the co-expression of ACh and glutamate in the developing and mature brain. Mapping markers of neurotransmitter phenotype solely in the adult brain might overlook neural systems that switch neurotransmitter phenotype during development, or use co-expression transiently in the wiring of developing circuits. Cholinergic signaling during development may be of special interest because of the significant evidence for adverse effects of developmental exposure to nicotine on postnatal brain function (Abbott & Winzer-Serhan, 2012). Thus we have taken an intersectional genetic strategy in the adult and developing mouse to explore the co-expression of cholinergic markers, including choline acetyltransferase (ChAT) and the vesicular acetylcholine transporter (VAChT), with VGluT2 in the subcortical brain. Expression of a tdTomato (tdT) reporter gene driven by Cre recombinase targeted to the *Chat* locus (Chat^{Cre}) identifies the known cholinergic systems, as well as unexpected populations of neurons in the subiculum, ventral thalamus, lateral hypothalamus, parabrachial nucleus, pontine gray, and medulla. Examination of ChAT protein and VAChT mRNA expression in the developing brain shows that all of these non-canonical cholinergic nuclei express these markers transiently during a phase of development when neural circuits are being established. Dual-recombinase intersectional labeling with Chat^{Cre} plus a transgenic strain expressing *flp* recombinase targeted to the *Slc17a6* locus (Vglut2^{Flp}), and a dual Cre-Flp dependent tdT reporter, demonstrates that all or nearly all of these transiently cholinergic neurons are glutamatergic in adulthood. The developmental expression of acetylcholine in these areas may identify previously unrecognized brain systems vulnerable to disruption by fetal or early postnatal exposure to nicotine or acetylcholinesterase inhibitors, and may help to explain the observed associations between maternal smoking and clinical problems including sudden infant death syndrome (SIDS) and neurocognitive deficits in early childhood.

MATERIALS AND METHODS

Animals.

The C*hat*$^{IRESCre::\Delta neo}$ (Chat^{Cre}) strain was obtained as a gift from Dr. Bradford Lowell, Harvard University. This strain is now available from the Jackson Laboratories (Jax #031661). The parent strain containing a neo resistance cassette (*Chat*$^{IRESCre::frt\text{-}neo\text{-}frt}$, Jax #006410) has been previously described (Rossi et al., 2011), and is referred to here as Chat^{CreNEO}. The mouse strain containing an IRES2-FlpO cassette targeted to the *Slc17a6* locus, Slc17a6$^{tm1.1(flpo)Hze/J}$, (Vglut2^{Flp}, Daigle et al., 2018), the Cre-dependent tdTomato

reporter strain *Gt(ROSA)26Sor*$^{tm14(CAG-tdTomato)Hze/J}$ (Ai14, Madisen et al., 2010), and the Cre/Flp-dependent tdTomato reporter strain *Gt(ROSA)26Sor*$^{tm65.1(CAG-tdTomato)Hze/J}$, (Ai65, Madisen et al., 2015) were obtained as gifts from Hongkui Zeng, Allen Institute for Brain Science. These transgenic strains are available from Jackson Laboratories as JAX #030212 (Vglut2^{Flp}), JAX #007914 (Ai14), and JAX #021875 (Ai65). All strains were maintained on a C57BL/6NCrl genetic background (Charles River).

Experimental design.

Heterozygous or homozygous Chat^{Cre} and Ai14 mice were interbred to produce double-transgenic Chat^{Cre}/Ai14 (Chat^{tdT}) mice. To generate triple-transgenic mice, the Chat^{Cre} and Vglut2^{Flp} strains were interbred to generate compound heterozygotes; these in turn were bred to Ai65 heterozygous or homozygous mice to produce Chat^{Cre}/Vglut2^{Flp}/Ai65 (Chat-Vglut2^{tdT}) mice expressing tdT only in cells which express, or have a developmental history of expressing, both ChAT and VGluT2. Adult mice of both sexes were used in these experiments and the sex of embryonic and early postnatal was not assessed.

Immunofluorescence and fluorescence in situ hybridization.

The brains of adult and early postnatal (P1–P7) developing mice were fixed by transcardial perfusion with 4% paraformaldehyde (PFA). The tissue was harvested, and adult brains were subsequently fixed for 4 hours, and postnatal brains for 2 hours, in 4% PFA. The tissue was then equilibrated in graded sucrose solutions to a final concentration of 30%, frozen at −80C in OCT solution, and cryosectioned at 25μm for imaging of endogenous fluorescence, immunofluorescence or in situ hybridization (Quina, Harris, Zeng, & Turner, 2017). Mouse embryos were harvested at E16.5 and E18.5. Embryos were decapitated, and the heads were fixed for 4 hours in PFA, followed by equilibration in graded sucrose and embedding at −80C in OCT solution. Embryonic tissue was sectioned at 16μm. Antisera for immunofluorescence include the following: Choline acetyltransferase (ChAT), goat polyclonal, EMD Millipore AB144P (Billerica, MA), RRID: AB_2079751, per the manufacturer, raised against human placental ChAT and affinity purified, it recognizes the expected band of 68–70kd on Western blots. In the adult mouse brain ChAT immunoreactivity was highly correlated with the expression of Chat mRNA. Red fluorescent protein (RFP), rabbit polyclonal, Rockland 600-401-379 (Limerick, PA), RRID: AB_2209751, per the manufacturer, raised against a fusion protein encoding full length RFP (234aa) derived from the mushroom polyp coral Discosoma. In the mouse brain this antibody was used to enhance the endogenous fluorescence of transgenically expressed tdTomato and no signal was detected in non-transgenic animals. Calcitonin Gene-Related Peptide (CGRP), rabbit polyclonal, EMD Millipore PC205L (Burlington, MA), RRID: AB_2068524; per the manufacturer, the antibody was raised against rat α-CGRP holopeptide (37AA), and staining in rat brain tissue is completely eliminated by pre-treatment of antibody with 10^{-5}M rat α-CGRP, but is not blocked by calcitonin. Ctip2, rat monoclonal 25B6, Abcam ab18465 (Cambridge, MA), RRID: AB_2064130; per the manufacturer, the immunizing antigen consists of amino acids 1–150 of CTIP2, and the antibody recognizes two expected bands of approximately 120kd on Western blots. Ctip2 immunoreactivity in the adult mouse brain was highly correlated with the pattern of Ctip2 mRNA expression. Guinea pig antiserum to Brn3a (Pou4f1) was prepared in the

investigator's laboratory against a fusion protein containing an 80 amino acid fragment of mouse Brn3a containing sequences N-terminal to the POU-specific domain that are not conserved across members of the Brn3 (POU4) gene class, was antigen-affinity purified before use, and does not give a signal in Brn3a null mouse embryos (RRID: AB_2576200, Quina et al., 2005).

Fluorescence *in situ* hybridization (FISH) was performed using RNAscope® Multiplex Fluorescent Assay v2 (Cat. No. 323100), according to manufacturer's instructions. Specific probes included Mm-Slc17a6 (319171), Mm-Chat-C2 (408731-C2), and tdTomato-C3 (317041-C3). Signal was developed with PerkinElmer TSA® Plus Fluorescein Kit (NEL741E001KT), Cyanine 3 Kit (NEL744E001KT), and Cyanine 5 Kit (NEL745E001KT). Fluorophores were used in 1:500 dilution. Tissue preparation and pretreatment were done according to the manufacturer's instructions for fresh frozen samples, which also worked well for PFA-fixed material prepared as described above. No difference in signal between fresh frozen and PFA-fixed tissue was observed using this protocol. Immunofluorescence and FISH images were acquired using Olympus VS120 Virtual Slide Microscope Scanner. The excitation/emission filter sets used for probe imaging were DAPI: 380–405/410–480, FITC: 460–490/500–550, Cy3/TRITC: 540–570/580–640, and Cy5: 625–645/655–705. Cell counting for expression and co-expression of genetic markers was performed using the Measurement and ROI toolbox of the Olympus OlyVIA 2.9 software. Expression levels were manually thresholded and only cells with nuclear profiles in the plane of section were counted. Laser scanning confocal imaging was performed Zeiss 710 34-channel Quasar LSC Microscope.

Database in situ hybridization data are derived from the following datasets from the Allen Institute for Brain Science Brain Atlas (Lein et al., 2007) and Developmental Brain Atlas (Thompson et al., 2014). Cases show coronal sections unless noted. Adult brain: Slc18a3 (VChAT), case 73521822; Tbr2, case 80516770. Developing brain: E18.5 Chat case 100059124; P4 Chat case 100059117; P4 VChAT sagittal case 100057395; P14 Slc17a6 (Vglut2) case 100042450; P14 Chat case 100045786; P14 Slc17a6 sagittal case 100026980; P14 Slc32a1 (Vgat), sagittal case 100076154. Complete datasets are available online at: http://mouse.brain-map.org/ and http://developingmouse.brain-map.org/.

RESULTS

Transgenic mapping of cholinergic neurons

Cholinergic neurons are characterized by co-expression of the biosynthetic enzyme for acetylcholine, choline acetyltransferase, together with the vesicular acetylcholine transporter (VAChT, Slc18a3) and the high affinity choline transporter (ChT, Slc5a7). The development of specific antibodies for ChAT has allowed the identification of groups of cholinergic neurons in the forebrain, tegmentum, and motor nuclei, and their efferent systems (Armstrong, Saper, Levey, Wainer, & Terry, 1983). In order to fate-map all neurons that express ChAT in the developing and mature brain, we used transgenic mice expressing Cre-recombinase targeted to the *Chat* gene locus (Figure 1a). This Cre driver strain is derived from a line which has been previously reported (Rossi et al., 2011), and used in several published studies (Chen et al., 2018; Hedrick et al., 2016; Li et al., 2018; Paez-Gonzalez,

Asrican, Rodriguez, & Kuo, 2014). However, the parent strain of these mice, widely distributed by a repository (*Chat*$^{IRESCre::frt\text{-}neo\text{-}frt}$, Jax 006410), contains a frt-NEO cassette, which was designed to be removed with Flp-mediated recombination prior to experimental use. In preliminary studies with these Chat^{CreNEO} mice, we frequently observed ectopic expression, for particularly in astrocytes, which do not normally express ChAT (data not shown). Similar results have been described by other investigators with this strain (Hedrick et al., 2016). An extensive characterization of behavior and ChAT expression has been performed in Chat^{CreNEO} mice (Chen et al., 2018), without considering the potential effects of the NEO cassette on gene expression. Subsequently we obtained a transgenic strain derived from this parent line, but with appropriate NEO excision (*Chat*$^{IRESCre::\Delta neo}$, Jax 031661, Figure 1a), and we have not observed ectopic expression using this Δneo strain with genetic reporters in C57BL/6 mice. The Δneo strain was thus used for all the experiments reported here and is identified simply as Chat^{Cre}.

To examine the brain-wide distribution of neurons that either express ChAT, or have expressed it developmentally, we interbred Chat^{Cre} mice with a reporter strain, Ai14, that conditionally expresses tdTomato from the Rosa26 gene locus (Figure 1b; Madisen et al., 2010), and effectively marks both neuronal cell bodies and their efferent fibers. Using this combinatorial system, we generated adult Chat^{Cre}/Ai14 (Chat^{tdT}) mice (N=3) and systematically compared the expression of tdTomato to the expression of VAChT mRNA reported in the Allen Brain Atlas database as an independent marker of cholinergic phenotype. The tdTomato reporter marked all recognized cholinergic cell populations in the mouse CNS. In the forebrain and diencephalon, labeled neurons included the ventral forebrain cholinergic system of the striatum and septum (Figure 1c–f), and the medial habenula and the arcuate nucleus of the hypothalamus (Figure 1g–i). Motor neurons were labeled at all brainstem levels (Figure 1j–v), including the oculomotor nuclei (3,4 and 6), the motor nuclei associated with the 5th, 7th, 10th, and 12th cranial nerves, and the nucleus ambiguus. Known cholinergic neurons were also labeled in the pedunculopontine tegmental nucleus and the laterodorsal tegmental nucleus (Figure 1m,n) and the preganglionic parasympathetic neurons associated with the superior and inferior salivatory nuclei (Figure 1p,q). Finally, although not usually discussed as brain cholinergic systems, some neurons expressing VAChT and tdT were observed in non-motor areas of the medulla, IRt and RVLM (Figure 1r,s). A subset of non-motor neurons with a sensory role in RVLM have been previously shown to exhibit ChAT expression in adult mice (Stornetta, Macon, Nguyen, Coates, & Guyenet, 2013), and cholinergic markers have been noted in a population of IRt neurons involved in regulating respiratory rhythms (T. M. Anderson et al., 2016).

Chat^{Cre} fate mapping reveals the unexpected expression of cholinergic markers in neurons not usually identified as cholinergic

Chat^{tdT} mice also showed extensive reporter expression in several sets of neurons in multiple brain regions that are not generally recognized as cholinergic, and which did not express detectable levels of ChAT protein in the adult brain. In the thalamus, tdTomato reporter expression was observed in the ventromedial subnucleus (Figure 2a,b). In the lateral hypothalamus, Chat^{tdT} neurons that were not immunoreactive for ChAT protein could be distinguished from cholinergic neurons in the adjacent substantia innominata, which were

immunoreactive for ChAT (Figure 2a,c). Fiber tracts and terminals were also observed in the hypothalamus and amygdala representing inputs from brainstem regions, discussed below (Figure 2d,e). In the cerebral cortex (Figure 2f,g), Chat^{tdT} mice showed reporter expression in scattered cells which have previously been shown to express low levels of ChAT, but are of uncertain neurotransmitter phenotype and function (Consonni, Leone, Becchetti, & Amadeo, 2009; von Engelhardt, Eliava, Meyer, Rozov, & Monyer, 2007). In the hippocampus, prominent labeling was observed in the subiculum at all rostrocaudal levels (Figure 2f,g,h,k), and fibers originating there were evident the medial mammillary nucleus (Figure 2i, Aggleton & Christiansen, 2015). At mesopontine levels, Chat^{tdT} signal was evident in the parabigeminal nucleus (Figure 2k,l), where low levels of ChAT immunoreactivity could also be detected (Figure 2m, a section adjacent to 2l), and in specific medial and lateral domains of the pontine gray (Figure 2n). ChAT immunoreactivity was not detectable in any of the Chat^{tdT} neurons described in Figure 2, except for the previously known forebrain cholinergic systems and low levels detected in the PBG, which has also previously been shown to express ChAT in the adult mouse (Mufson, Martin, Mash, Wainer, & Mesulam, 1986).

More caudally, in the pontine tegmentum, Chat^{tdT} expression was observed in the lateral parabrachial (LPB) and Kölliker-Fuse (KF) nuclei of the parabrachial complex (Figure 3a, b). The LPB is known to project to the hypothalamus and amygdala, probably accounting for the tdT-labeled fiber terminals observed in these regions (Figure 2d,e, also see discussion). Expression was also observed the periolivary region (PO, Figure 3c). More caudally, in a ventral position, neurons expressing Chat^{tdT} appear in RVLM (Figure 3d,e). tdT-labeled neurons were also noted in the lateral part of the inferior olive (IO, Figure 3f,g). Identification of these neurons as part of the IO complex was verified by immunofluorescence for the transcription factor Pou4f1/Brn3a, a known IO marker (Figure 3h, Fedtsova & Turner, 1995). Dense Chat^{tdT} expression was also observed in the gracile and cuneate nuclei (Figure 3i,j).

ChAT-expressing neurons in the adult mouse brain have also been reported to have a non-canonical role in adult subventricular zone (SVZ) neurogenesis (Paez-Gonzalez et al., 2014). In this study the Cre driver line Chat^{CreNEO} (Jax 006410), was combined with a Cre-dependent *Gt(ROSA)26*-targeted tdTomato reporter strain similar but not identical to the strain used here (Arenkiel et al., 2011) to identify a “previously unknown population of ChAT^{+} neurons residing in and innervating the SVZ niche”. Although the SVZ is adjacent to the caudate nucleus of the striatum, which has an intrinsic population of ChAT-expressing neurons, these specialized cells were reported to be in the subependymal zone outside the striatal compartment. In adult mice, the location of the SVZ is readily recognized by the ongoing expression of the developmental transcription factor Tbr2 (Figure 4a–c), which is required for the normal neurogenesis in the SVZ and rostral migratory stream (Kahoud, Elsen, Hevner, & Hodge, 2014), contributing multiple cell types to the olfactory bulb (Mihalas & Hevner, 2017). The majority of neurons in the adjacent striatum are medium spiny neurons (MSNs) which express the nuclear factor Ctip2 (Arlotta, Molyneaux, Jabaudon, Yoshida, & Macklis, 2008), while the intrinsic striatal cholinergic neurons are Ctip2 negative, and are scattered among the MSN population (Figure 4d,e). To search for the reported cholinergic neurons within the SVZ, we examined both hemispheres of the entire

SVZ neurogenic zone of Chat^{tdT} mice (N=3), aged 5 months (mature adult, N=2, 16 sections each) and 5 weeks (adolescent, N=1, 12 sections), at 100μm intervals corresponding to the adult coordinates bregma 1.8 to bregma 0.0. No tdT-expressing neurons were observed in the SVZ at any level in adult animals (Figure 4d–e), and all tdT-expressing striatal neurons were completely surrounded by Ctip2-expressing MSNs. In order to ensure that the Chat^{tdT} mice were accurately reporting ChAT expression, we also performed immunofluorescence for ChAT protein in adjacent sections, but again observed no neurons in the SVZ (Figure 4f,g). Finally, we considered the possibility that a ChAT-expressing population of SVZ neurons might be present in young animals, and disappear with age. However, as in the adult, no tdT-expressing neurons were observed in the SVZ at 5 weeks of age (Figure 4h–j). Because the original report did not describe the number or anatomical distribution of the reported SVZ cholinergic neurons, it is difficult to make a direct comparison with our results, but we see no evidence for a population of ChAT-expressing neurons in the SVZ, distinct from striatal cholinergic neurons. One possible explanation for the prior results may be ectopic reporter expression driven by Chat^{CreNEO}, since this has been observed in other brain areas.

Cholinergic markers are transiently expressed in developmental windows specific for each cell type

It is remarkable that Chat^{Cre} induces tdT reporter expression in multiple brain regions that do not express levels of ChAT protein detectable by immunofluorescence or ChAT mRNA detectable by *in situ* hybridization in the adult mouse, including the subiculum, ventral thalamus, pretectum, pons, parabrachial system, inferior olive and cuneate/gracile nuclei. Since Cre-mediated recombination of the *Rosa26* reporter locus permanently activates tdTomato expression, these results suggest that ChAT is expressed transiently in these areas, and that these neurons subsequently assume a different neurotransmitter phenotype. However, it is also possible that the Chat^{Cre} driver induces ectopic expression of the reporter gene in neurons that do not normally express it. To confirm the developmental expression of ChAT protein in these areas, we examined normally developing embryonic (N=4, harvested at E16.5–E18.5), and early postnatal Chat^{tdT} mice (N=5, harvested at P1–P7). Developing brains were examined at 100μm intervals throughout the neural axis from the diencephalon to the medulla. In each area, we determined the developmental time of onset of Chat^{tdT} expression and the window of ChAT protein expression with respect to the developmental program of the cell type in question. In this developmental series, Chat^{tdT}-labeled neurons appeared according to the distinct timetable of neural differentiation in each area. However, in each developing embryo or pup, the expression pattern of tdT was completely consistent with the ultimate pattern of expression observed in the adult Chat^{tdT} brains.

In the VM a group of Chat^{tdT} neurons, also immunoreactive for ChAT protein, was clearly evident at P4 (Figure 5a,b). In the LH, Chat^{tdT} neurons were also evident at P4, and ChAT immunoreactivity was present, but was less intense than in neurons of the adjacent substantia innominata (SI, Figure 5a,c). Chat^{tdT}-expressing neurons were first noted in the subiculum at P4 (Figure 5d). ChAT protein expression was detectable there (Figure 5e), but at much lower levels than in known cholinergic centers, such as the MHb (Figure 5f). Chat^{tdT}-expressing neurons were more numerous in the subiculum by P7 (Figure 5g). Neurons of the reticular nucleus of the pons and the central pontine gray (together referred

to here as the pontine nucleus) originate in the secondary precerebellar neuroepithelium of the rhombic lip, and migrate via the anterior extramural migratory stream to settle in the pons by E20 in the rat (Altman & Bayer, 1987). This is approximately equivalent to E18.5 in the mouse, and this migration is essentially complete at the time of birth. Few Chat^{tdT}-expressing or ChAT immunolabeled cells were noted In the region of the presumptive pontine nucleus at E16.5 and E18.5, or along this migratory route (data not shown). Thus it seems unlikely that ChAT is expressed in these cells during this migratory phase. By P1, Chat^{tdT}-expressing neurons were evident in the pontine nucleus, and exhibited low levels of ChAT protein expression (Figure 5h,i). At P4, ChAT protein signal was stronger in the tdT-labeled neurons in the central part of the pontine nucleus, and was already fading in the lateral part (Figure 5j). Also by P4, the first Chat^{tdT}-labeled mossy fibers were evident in the middle cerebellar peduncle and developing paraflocculus (PFl, Figure 5k). In the PBG, ChAT protein expression was evident at E16.5, and Chat^{tdT} expression was robust from E18.5 onward (Figure 5l–n).

In the mesopontine tegmentum, a few neurons expressing ChAT protein and Chat^{tdT} were evident in the LDTg and LPB at E16.5 (data not shown). At E18.5, neurons with varying levels of marker co-expression could be discerned in both nuclei (Figure 6a–c). Parabrachial fibers expressing Chat^{tdT} and ChAT immunoreactivity were evident in the Ce by P1 (Figure 6d). In the medulla, strong expression of ChAT protein was observed in Chat^{tdT} labeled neurons in IRt at P4 (Figure 6e,f). Neurogenesis in the cuneate/gracile nuclei occurs early, and is complete by E15 in the rat (mouse ~E13.5, Altman & Bayer, 1980). Weak expression of ChAT protein was detected in the cuneate at E16.5 (data not shown), and ChAT and Chat^{tdT} signals were strong at E18.5 (Figure 6g,h) and P1 (Figure 6i). At P4, in sections through the diencephalon (Figure 6j–m), co-expression of ChAT protein and Chat^{tdT} were clearly seen in the MHbV and fasciculus retroflexus (Figure 6k). Fibers originating from the cuneate/gracile nuclei in VPL co-express ChAT protein and tdT at this stage (Figure 6l), while ChAT protein expression in the LPB projection to the amygdala shows diminished ChAT immunoreactivity compared to P1 (Figure 6m).

Additional insight into the transient expression of cholinergic markers in these brain regions can be gained from an existing gene expression database for the developing mouse brain (Thompson et al., 2014), which includes ISH data for the cholinergic markers ChAT and VAChT at several embryonic and postnatal stages. Figure 7 summarizes the earliest available stages at which these markers showed clear, robust expression. ChAT mRNA was detected at postnatal day 4 (P4) in the ventromedial thalamus (Figure 7a–c), and in the subiculum Figure 7d–f). Examination of embryonic day 18.5 (E18.5) embryos confirmed ChAT mRNA expression in the PBG and pons (Figure 7g–i), the parabrachial complex (Figure 7j–k), and the gracile and cuneate nuclei (Figure 7l–m). VAChT expression was also noted in the pontine nucleus at P4 (Figure 7h–i), confirming that these transiently ChAT-expressing neurons have the potential to use acetylcholine as a synaptic transmitter at this developmental stage.

Most or all of the transiently cholinergic neurons are ultimately glutamatergic

In regions where neurons with transient expression of ChAT mRNA are densely clustered, it is possible to determine the ultimate neurotransmitter phenotype of these neurons by examining mRNA expression after ChAT is no longer expressed. At P14 ChAT mRNA was no longer detected by ISH in the pontine nucleus, and VGluT2 was expressed throughout (Figure 8a,b). As the GABAergic marker Vgat is not expressed in the pontine area (Figure 8c,d), we conclude that the transiently ChAT-expressing pontine neurons assume an exclusively glutamatergic phenotype. ChAT mRNA was also no longer detected in the gracile and cuneate nuclei at P4, and these neurons also assume a glutamatergic phenotype (Figure 8e,f). In contrast, at this stage, the PBG continues to co-express ChAT and VGluT2 (Figure 8a,b).

In order to examine the entire brain for neurons that co-express ChAT and VGluT2, including neurons with transient expression of either gene, we adopted an intersectional fate mapping strategy using a Rosa26-targeted reporter strain, Ai65, which requires the excision of two tandem transcriptional stop sequences, flanked by frt and loxP sites, to activate a tdTomato reporter (Figure 9a). Mice were interbred to produce triple transgenic $Chat^{Cre}$/$Vglut2^{FlpO}$/Ai65 offspring (Chat-$Vglut2^{tdT}$, N=4 adult animals), and the entire neural axis was examined for expression of the transgenic tdTomato marker. In each of the brain areas described below, concordant expression was observed in 3/3 specimens sectioned in coronal plane, and an additional case sectioned in the sagittal plane.

As expected, Chat-$Vglut2^{tdT}$ neurons were a subset of the $Chat^{tdT}$ neurons identified in Figures 1–3. However, many known cholinergic neurons showed no expression of Chat-$Vglut2^{tdT}$. This was verified by immunostaining Chat-$Vglut2^{tdT}$ brain samples for ChAT protein expression across the entire CNS. ChAT-immunoreactive, Chat-$Vglut2^{tdT}$-negative neurons included the forebrain cholinergic neurons in the septum and diagonal band, caudate/putamen, ventral striatum, and substantia innominata (data not shown). Likewise, no tdTomato expression was observed in the scattered cortical neurons seen in $Chat^{tdT}$ mice (Figure 2g and data not shown), but the Chat-$Vglut2^{tdT}$ transgene may not be informative for these neurons, since the cerebral cortex predominantly expresses the vesicular glutamate transporter VGluT1, not VGluT2. Brainstem motor neurons were also negative for Chat-$Vglut2^{tdT}$, including the neurons of the oculomotor system (associated with cranial nerves 3,4 and 6), the trigeminal motor nucleus (Mo5), the facial motor nucleus (7), the nucleus ambiguus, the facial motor nucleus (10) and the hypoglossal motor nucleus (12).

At the level of the diencephalon, Chat-$Vglut2^{tdT}$-expressing neurons were observed in the VM thalamus and rostral LH (Figure 9b–d). As expected, the MHbV, known to co-express glutamate and acetylcholine in adult mice, was labeled with tdTomato (Figure 9e,g), as were MHbV efferents in the fasciculus retroflexus. Chat-$Vglut2^{tdT}$-expressing neurons were also found in the subiculum, and fibers originating there projected to the mammillary hypothalamus (MM, Figure 2f,h). In the rostral midbrain, a small population of neurons of unknown function were labeled in the pretectum (Figure 9h), whereas in the retinorecipient layers of the superior colliculus (SC) tdTomato was observed in afferent fibers only, originating in the retina and projecting to the SC via the optic tract (Figure 9e). In the mesopontine area, Chat-$Vglut2^{tdT}$ expression strongly resembled that seen with $Chat^{Cre}$

alone, with robust labeling of the PBG (Figure 9i,j). Previous studies have also shown ChAT expression in the adult PBG, or cholinergic C8 group (Mufson et al., 1986). However, the co-expression of glutamate by PBG neurons does not appear to have been previously recognized. Thus the PBG is the only example identified here of VGluT2 expression in a group of neurons previously known to be cholinergic; in all other cases we have described cholinergic markers in neurons that are generally known as glutamatergic. In the pontine gray, Chat-Vglut2^{tdT} was extensively expressed in in medial and lateral zones, following the pattern of Chat^{Cre}-driven expression (Figure 9i,k,l), with extensive mossy fiber labeling in the cerebellar hemispheres (Figure 9m).

In the mesopontine tegmentum, neurons in the LDTg showed a mixed phenotype. A majority of ChAT-immunoreactive neurons were negative for Chat-Vglut2^{tdT}, but a subpopulation in the ventrolateral LDTg were ChAT immunoreactive (Figure 10a,b). This appears to be consistent with a subpopulation of PPTg and LDTg ChAT/VGluT2 co-expressing neurons recently identified by *in situ* hybridization (Luquin, Huerta, Aymerich, & Mengual, 2018), although the abundance of such neurons has differed between investigators (Wang & Morales, 2009). Neurons in the LPB also expressed Chat-Vglut2^{tdT} (Figure 10a,c). Many of these LPB neurons co-expressed the neuropeptide CGRP, and strong co-localization of CGRP and tdT could be observed in the central amygdala, to which CGRP-expressing LPB neurons are known to project (Figure 10d,e; Palmiter, 2018). Some tdTomato labeled neurons were also noted in the Kölliker-Fuse region within the parabrachial complex.

In the rostral medulla, Chat-Vglut2^{tdT} expressing neurons were observed in IRt and RVLM (Figure 10f–h). Most of these neurons had detectable ChAT immunoreactivity, albeit at lower levels than the adjacent motor neurons of the nucleus ambiguus. Some neurons in the lateral part of the IO also expressed tdT (Figure 10f,i). In the caudal medulla, expression of Chat-Vglut2^{tdT} in the cuneate and gracile nuclei (Figure 10i,j) was similar to that seen in Chat^{tdT} mice, indicating that all or nearly all of these transiently ChAT-expressing neurons are ultimately glutamatergic. Ascending tdTomato-labeled fibers from the cuneate/gracile nuclei could be seen to traverse the brainstem and project rostrally via the medial lemniscus (Figure 10i).

Although Chat-Vglut2^{tdT} expression was observed in all of the brain regions with unexpected Chat^{tdT} signal, we also wished to confirm that these neurons have a glutamatergic phenotype in the adult brain, that is, that they do not express both ChAT and VgluT2 transiently, then assume some other phenotype. To accomplish this, and also to confirm that the Vglut2^{Flp} induction of the tdTomato genetic reporter marked glutamatergic neurons with high fidelity, we examined the cellular localization of tdT with endogenous VgluT2 in the adult brain. Unlike ChAT, VgluT2 is not well suited to cellular localization by immunostaining. Thus in the genetically labeled Chat-Vglut2^{tdT} neurons, we used fluorescence *in situ* hybridization (FISH, RNAscope) to examine VgluT2 and tdTomato co-expression (Figure 11). FISH results confirmed that Chat-Vglut2^{tdT} neurons have a glutamatergic phenotype in all areas examined in the adult brain, including the MHbV examined as a positive control (Figure 11a), subiculum (65/66 tdT-expressing neurons in 9 sections also expressed Vglut2, Figure 11b,c), ventromedial thalamus (18/18 co-expressing

neurons in 3 sections, Figure 11d), pretectum (43/43 co-expressing neurons in 6 sections, Figure 11e,f), pontine nucleus (1454/1469 co-expressing neurons in 9 sections, Figure 11g,g), PBG (565/565 co-expressing neurons in 6 sections, Figure 11i), IRt (125/131 co-expressing neurons in 5 sections, Figure 1j,k), inferior olive (139/157 co-expressing neurons in 6 sections, Figure 11l,m), and cuneate/gracile nuclei (430/430 co-expressing neurons in 4 sections, Figure 11n,o).

Glutamatergic neurons that express Chat-Vglut2^{tdT} in the adult brain record the entire cellular history of Chat^{Cre} and Vglut2^{Flp} expression. Thus these neurons could express ChAT before the onset of VgluT2 expression in development, or simultaneously with it, consistent with a neuromodulator role for ACh. In order to determine the timing of ChAT and VgluT2 expression in the brainstem nuclei marked by Chat-Vglut2^{tdT}, we used FISH for ChAT and VgluT2 mRNA near the developmental onset of Chat^{tdT} expression in these neurons. We also used a tdTomato mRNA probe to co-localize tdT and VgluT2 mRNAs in Chat^{tdT} mice. In the pontine nucleus at E18.5, ChAT and VgluT2 mRNA are both expressed, and appear to be co-localized, although the punctate nature of the FISH signal and the densely compacted cell bodies in this area did not allow exact co-localization of the signals within distinct cellular profiles (Figure 12a,b). Co-expression of ChAT and VgluT2 persisted in the pontine nucleus at P1 (Figure 12c). In the PBG at E18.5, co-expression of ChAT and VgluT2 was also evident, and contrasted with the discrete expression of these markers in the oculomotor (3) nucleus and the surrounding PAG, imaged under the same conditions in the same section (Figure 12d,e). Imaging Chat^{tdT} mRNA expression with VgluT2 mRNA gave a similar result (Figure 12f). In the PBG at P1, ChAT and VgluT2 were co-expressed, with better definition of cellular profiles compared to E18.5 (Figure 12g). In the LPB at P1, shortly after the onset of ChAT expression, VgluT2 mRNA was detectable, but weak in comparison to surrounding glutamatergic neurons (Figure 12h), and similar results were seen with tdT/VgluT2 expression (Figure 12i). In the LPB at P4, co-expression of ChAT and VgluT2 was observed in clear cellular profiles (Figure 12j), in contrast to the largely distinct expression of these markers in the LDTg in the same tissue section (Figure 12k). Co-expression of ChAT and VgluT2 was also observed in the gracile and cuneate nuclei at E18.5, in contrast to the nucleus of the solitary tract (Sol) and the motor nucleus of the vagus nerve (10), which only expressed VgluT2 and ChAT, respectively (Figure 12l,m). A similar pattern of co-expression was observed for tdT and VgluT2 (Figure 12n). Taken together, these results indicate that these groups of neurons do not go through an exclusively cholinergic phase of development, with a “switch” from cholinergic to glutamatergic phenotype, but instead are consistently glutamatergic neurons with transient developmental co-expression of the systems for the biosynthesis and synaptic packaging of acetylcholine.

DISCUSSION

Here we have shown that the co-expression of acetylcholine and glutamate in CNS neurons is much more common than previously appreciated, especially during the period of development when circuits are established. Populations of glutamatergic neurons in brain areas relevant to cognition, motor control, arousal in response to distress, and respiration express ChAT and VAChT during specific developmental windows, but lose their cholinergic phenotype by adulthood. We have also identified groups of neurons in the PBG and medulla

that have “habenula-like” persistent co-expression of cholinergic and glutamatergic markers. The developmental course of cholinergic gene expression in all of these areas is summarized in Figure 13. These findings significantly expand the range of neurons that co-express ACh with markers of other fast neurotransmitter systems, which is known to include striatal cholinergic neurons that express VGluT3 (Boulland et al., 2004; Gras et al., 2002; Higley et al., 2011), and ACh/GABA co-expressing neurons that have been identified in the adult forebrain cholinergic system and in the retina (Granger et al., 2016; Saunders et al., 2015).

The co-expression of ChAT with VAChT suggests that acetylcholine is synaptically packaged in these transiently cholinergic neurons, rather than used in a non-canonical role, for instance as a signal in neurogenesis or cell migration. Specifically, we found no evidence for a previously reported population of ChAT-expressing cells in the SVZ neurogenic niche (Paez-Gonzalez et al., 2014). Instead, ChAT and VAChT are expressed after neurogenesis is complete and efferent axons are observed in target nuclei. This suggests that ACh plays a role in the establishment or refinement of glutamatergic synaptic connections in several important pathways, including the projection of the subiculum to the mammillary hypothalamus, the pontocerebellar system, the projection of the LPB to the amygdala, and the cuneate/gracile nuclei to the thalamus.

Cholinergic modulation and the development of glutamatergic synapses.

ACh released by the developing brain systems identified here could function either as a neuromodulator, stimulating extrasynaptic cholinergic receptors (Picciotto, Higley, & Mineur, 2012), or as a ‘fast’ neurotransmitter (Roerig, Nelson, & Katz, 1997), but the timing of expression in these systems strongly suggests a neuromodulator role. The effects of ACh on the development and plasticity of glutamatergic transmission has been examined primarily in the hippocampus and cortex (Gu, Lamb, & Yakel, 2012; Gu & Yakel, 2011; Halff, Gomez-Varela, John, & Berg, 2014; Lozada et al., 2012a, 2012b), which receive major heterosynaptic cholinergic inputs from the septum and forebrain cholinergic system, respectively (Gu & Yakel, 2011; Wu, Williams, & Nathans, 2014). The co-expression of ACh and glutamate in developing neurons would allow ACh to act homosynaptically in synapse formation and maturation. The habenulopeduncular pathway is the best-understood example of homosynaptic ACh release at a synapse that uses glutamate as its principal transmitter (Frahm et al., 2015; Hsu et al., 2013; Ren et al., 2011; Soria-Gomez et al., 2015). However, ChAT expression persists in the adult MHb, and it is unclear if it will be a model for the function of homosynaptically released ACh in the developing circuits identified here.

Developmental expression of ACh can permit a short-cut to synaptic maturity during a time when ‘silent’ synapses are prevalent (Hanse, Seth, & Riebe, 2013; Rumpel, Kattenstroth, & Gottmann, 2004; Xiao, Wasling, Hanse, & Gustafsson, 2004). These immature synapses cannot effectively communicate a glutamatergic signal until a $Ca2^{+}$ signal recruits AMPA glutamate receptors (Hanse et al., 2013). Either of the two major subfamilies of cholinergic receptors could provide a $Ca2^{+}$ signal, as nicotinic receptors are acetylcholine-gated $Ca2^{+}$-permeable ion channels (Dwyer, McQuown, & Leslie, 2009) and muscarinic receptors are G-protein coupled and capable of triggering intracellular waves of $Ca2^{+}$ release (Rathouz, Vijayaraghavan, & Berg, 1995; Thiele, 2013). Both subfamilies are found at high levels

during development (Fiedler, Marks, & Collins, 1987; Hohmann, Pert, & Ebner, 1985; X. Zhang, Liu, Miao, Gong, & Nordberg, 1998; Zoli, Le Novere, Hill, & Changeux, 1995). The glutamatergic circuits in the hippocampus, cortex, and brainstem known to be modulated by ACh are permanently altered by developmental disruption of cholinergic receptors through genetic deletion or exposure to nicotine (Bailey, Tian, Kang, O'Reilly, & Lambe, 2014; Ballesteros-Yanez, Benavides-Piccione, Bourgeois, Changeux, & DeFelipe, 2010; Baumann & Koch, 2017; Kang, Tian, Bailey, & Lambe, 2015; Liang et al., 2006; Y. Zhang, Hamilton, Nathanson, & Yan, 2006). The dual ChAT/Vglut2-expressing pathways identified here suggest that such effects will impact several other brain systems using homosynaptic mechanisms, potentially expanding the scope of nicotine as a developmental disruptor.

Some prior evidence also supports a role for ACh in the developing pontocerebellar system, where the application of exogenous ACh and nicotine can enhance both glutamatergic and GABAergic synaptic currents in Purkinje cells in a developmental window from P5–P10 (Kawa, 2002). However, the endogenous source of ACh that mediates this age-specific effect is unknown. Even in adult rodents, there is only sparse innervation to the cerebellum from known cholinergic areas (Jaarsma et al., 1997; Stornetta et al., 2013; Y. Zhang, Kaneko, Yanagawa, & Saito, 2014). Here we have shown that in the developing central pontine nucleus, ChAT expression peaks in the postnatal window during which ACh enhances cerebellar synaptic strength, suggesting that the pontine mossy fibers themselves may be a developmental source of ACh.

Clinical implications: Risks of smoking during pregnancy.

A significant body of epidemiological evidence has linked maternal smoking during pregnancy to poor outcomes after birth, particularly low birth weight and SIDS (Abbott & Winzer-Serhan, 2012; T. Anderson et al., 2018; Hakeem, Oddy, Holcroft, & Abenhaim, 2015; K. Zhang & Wang, 2013). Maternal smoking is also associated with neuropsychiatric problems in offspring, including behavioral disorders and impairment of sensory processing and cognition (Bryden et al., 2016; Clifford, Lang, & Chen, 2012; Liang et al., 2006; Linnet et al., 2003), although the weight of nicotine exposure versus other factors remains unclear (Gustavson et al., 2017; Lindblad & Hjern, 2010; Tiesler & Heinrich, 2014). Disruption of cholinergic signaling in development could also underlie the harmful developmental effects of organophosphate (OP) insecticides, such as chlorpyrifos, which act as inhibitors of acetylcholinesterase (Burke et al., 2017), and which have and been associated with cognitive, motor and behavioral effects in children (Gonzalez-Alzaga et al., 2014).

A major contributor to SIDS is the failure to arouse in response to hypoxic and hypercapnic conditions (Garcia, Koschnitzky, & Ramirez, 2013), which may occur when babies sleep in the prone position (Horne, Franco, Adamson, Groswasser, & Kahn, 2002). Much work on the neuropathology of SIDS has focused on the role of brainstem serotonin signaling (Haynes et al., 2017; Kinney, Richerson, Dymecki, Darnall, & Nattie, 2009), and the link to chemosensation (Buchanan, Smith, MacAskill, & Richerson, 2015; Ray et al., 2011), the hypoxic response of the respiratory network (J. M. Ramirez, Folkow, & Blix, 2007; S. Ramirez et al., 2016; Tryba, Pena, & Ramirez, 2006) and arousal (Buchanan & Richerson, 2010; Iwasaki et al., 2018; Mateika, Komnenov, Pop, & Kuhn, 2018). Yet many aspects of

cardiorespiratory control also depend on cholinergic mechanisms, and are altered by nicotine exposure (Cerpa et al., 2015; Shao & Feldman, 2009; Vivekanandarajah, Waters, & Machaalani, 2019), including the respiratory chemosensory response (Coddou, Bravo, & Eugenin, 2009; Eugenin et al., 2008), and multiple aspects of upper airway control (Cholanian, Powell, Levine, & Fregosi, 2017; Cholanian, Wealing, Levine, & Fregosi, 2017; Powell, Levine, Frazier, & Fregosi, 2015; Wollman, Levine, & Fregosi, 2018). Chat-Vglut2^{tdT} expression identifies two known groups of cholinergic/glutamatergic neurons in the medulla, located in IRt and RVLM. Both populations continue to express ChAT in the adult brain, but seem to function primarily as glutamatergic neurons. The IRt neurons coincide with the so-called post-inspiratory complex (PiCo, T. M. Anderson et al., 2016), the role of these neurons in arousal from respiratory distress has not been examined. The cholinergic/glutamatergic RVLM neurons appear to be involved in sensory processing rather than respiratory control (Stornetta et al., 2013).

Developmental expression of ChAT identifies two other areas that are involved in respiratory control and arousal, the LPB and cerebellum/precerebellar system, not previously considered as targets for the effects of nicotine *in utero*. In rodents, the LPB CGRP neurons convey multiple signals that cause alarm or distress (Palmiter, 2018), including hypercapnia (Yokota, Kaur, VanderHorst, Saper, & Chamberlin, 2015). Glutamatergic signaling is required for this response (Kaur et al., 2013), and activation of the LPB CGRP neurons promotes wakefulness, while optogenetic inhibition of LPB terminals in the LH, CeA, or basal forebrain blunts the arousal response to hypercapnia (Kaur et al., 2017). If acetylcholine is involved in the development of these glutamatergic neurons, exposure of these pathways to nicotine *in utero* could be an important mechanistic link in the association between maternal smoking, disturbed arousal, and SIDS (Horne, Franco, Adamson, Groswasser, & Kahn, 2004).

In summary, we have used genetic fate mapping, together with confirmatory protein and RNA expression studies across developmental time, to identify multiple populations of neurons not previously known to be cholinergic during development. Intersectional fate mapping demonstrates that these neurons are also glutamatergic, and the time course of cholinergic expression suggests that ACh acts as a neuromodulator during development of excitatory circuits. These novel populations of developmentally cholinergic neurons are found in brain areas relevant to cognition, motor control, arousal in response to distress, and respiration. Their existence and the timing of their cholinergic phenotype raise questions about specific circuits that may be more vulnerable to disruption by nicotine exposure *in utero* than previously imagined, and thus suggest new mechanisms for the adverse neonatal and childhood outcomes initiated by prenatal nicotine exposure.

Acknowledgements

We thank Dr. Hongkui Zeng and the Allen Institute for Brain Science for transgenic mice and access to unpublished data. We also thank Drs. Rebecca Hodge and Robert Hevner for helpful discussion of adult neurogenesis, Dr. Richard Palmiter for guidance on the analysis of the parabrachial nucleus, and Drs. Eric Knudsen and John Huguenard for helpful discussions of the parabigeminal nucleus.

REFERENCES

Abbott LC, & Winzer-Serhan UH (2012). Smoking during pregnancy: lessons learned from epidemiological studies and experimental studies using animal models. Crit Rev Toxicol, 42(4), 279–303. doi:10.3109/10408444.2012.658506 [PubMed: 22394313]

Aggleton JP, & Christiansen K (2015). The subiculum: the heart of the extended hippocampal system. Prog Brain Res, 219, 65–82. doi:10.1016/bs.pbr.2015.03.003 [PubMed: 26072234]

Altman J, & Bayer SA (1980). Development of the brain stem in the rat. I. Thymidine-radiographic study of the time of origin of neurons of the lower medulla. J Comp Neurol, 194(1), 1–35. [PubMed: 7440792]

Altman J, & Bayer SA (1987). Development of the precerebellar nuclei in the rat: IV. The anterior precerebellar extramural migratory stream and the nucleus reticularis tegmenti pontis and the basal pontine gray. J Comp Neurol, 257(4), 529–552. [PubMed: 3693597]

Anderson T, Lavista Ferres J, Ren S, Moon R, Goldstein R, Ramirez J, & Mitchell E (2018). Maternal smoking before and during pregnancy and the risk of sudden unexpected infant death. Pediatrics, in press(in press).

Anderson TM, Garcia AJ 3rd, Baertsch NA, Pollak J, Bloom JC, Wei AD, … Ramirez JM (2016). A novel excitatory network for the control of breathing. Nature, 536(7614), 76–80. doi:10.1038/nature18944 [PubMed: 27462817]

Arenkiel BR, Hasegawa H, Yi JJ, Larsen RS, Wallace ML, Philpot BD, … Ehlers MD (2011). Activity-induced remodeling of olfactory bulb microcircuits revealed by monosynaptic tracing. PLoS One, 6(12), e29423. doi:10.1371/journal.pone.0029423 [PubMed: 22216277]

Arlotta P, Molyneaux BJ, Jabaudon D, Yoshida Y, & Macklis JD (2008). Ctip2 controls the differentiation of medium spiny neurons and the establishment of the cellular architecture of the striatum. J Neurosci, 28(3), 622–632. doi:10.1523/JNEUROSCI.2986-07.2008 [PubMed: 18199763]

Armstrong DM, Saper CB, Levey AI, Wainer BH, & Terry RD (1983). Distribution of cholinergic neurons in rat brain: demonstrated by the immunocytochemical localization of choline acetyltransferase. J Comp Neurol, 216(1), 53–68. doi:10.1002/cne.902160106 [PubMed: 6345598]

Bailey CD, Tian MK, Kang L, O'Reilly R, & Lambe EK (2014). Chrna5 genotype determines the long-lasting effects of developmental in vivo nicotine exposure on prefrontal attention circuitry. Neuropharmacology, 77, 145–155. doi:10.1016/j.neuropharm.2013.09.003 S0028–3908(13)00410–3 [pii] [PubMed: 24055499]

Ballesteros-Yanez I, Benavides-Piccione R, Bourgeois JP, Changeux JP, & DeFelipe J (2010). Alterations of cortical pyramidal neurons in mice lacking high-affinity nicotinic receptors. Proc Natl Acad Sci U S A, 107(25), 11567–11572. doi:10.1073/pnas.1006269107 [PubMed: 20534523]

Baumann VJ, & Koch U (2017). Perinatal nicotine exposure impairs the maturation of glutamatergic inputs in the auditory brainstem. J Physiol, 595(11), 3573–3590. doi:10.1113/JP274059 [PubMed: 28190266]

Boulland JL, Qureshi T, Seal RP, Rafiki A, Gundersen V, Bergersen LH, … Chaudhry FA (2004). Expression of the vesicular glutamate transporters during development indicates the widespread corelease of multiple neurotransmitters. J Comp Neurol, 480(3), 264–280. doi:10.1002/cne.20354 [PubMed: 15515175]

Bryden DW, Burton AC, Barnett BR, Cohen VJ, Hearn TN, Jones EA, … Roesch MR (2016). Prenatal Nicotine Exposure Impairs Executive Control Signals in Medial Prefrontal Cortex. Neuropsychopharmacology, 41(3), 716–725. doi:10.1038/npp.2015.197 [PubMed: 26189451]

Buchanan GF, & Richerson GB (2010). Central serotonin neurons are required for arousal to CO2. Proc Natl Acad Sci U S A, 107(37), 16354–16359. doi:10.1073/pnas.1004587107 [PubMed: 20805497]

Buchanan GF, Smith HR, MacAskill A, & Richerson GB (2015). 5-HT2A receptor activation is necessary for CO2-induced arousal. J Neurophysiol, 114(1), 233–243. doi:10.1152/jn.00213.2015 [PubMed: 25925320]

Burke RD, Todd SW, Lumsden E, Mullins RJ, Mamczarz J, Fawcett WP, … Albuquerque EX (2017). Developmental neurotoxicity of the organophosphorus insecticide chlorpyrifos: from clinical

findings to preclinical models and potential mechanisms. J Neurochem, 142 Suppl 2, 162–177. doi:10.1111/jnc.14077 [PubMed: 28791702]

Cerpa VJ, Aylwin Mde L, Beltran-Castillo S, Bravo EU, Llona IR, Richerson GB, & Eugenin JL (2015). The Alteration of Neonatal Raphe Neurons by Prenatal-Perinatal Nicotine. Meaning for Sudden Infant Death Syndrome. Am J Respir Cell Mol Biol, 53(4), 489–499. doi:10.1165/rcmb.2014-0329OC [PubMed: 25695895]

Chen E, Lallai V, Sherafat Y, Grimes NP, Pushkin AN, Fowler JP, & Fowler CD (2018). Altered Baseline and Nicotine-Mediated Behavioral and Cholinergic Profiles in ChAT-Cre Mouse Lines. J Neurosci, 38(9), 2177–2188. doi:10.1523/JNEUROSCI.1433-17.2018 [PubMed: 29371319]

Cholanian M, Powell GL, Levine RB, & Fregosi RF (2017). Influence of developmental nicotine exposure on glutamatergic neurotransmission in rhythmically active hypoglossal motoneurons. Exp Neurol, 287(Pt 2), 254–260. doi:10.1016/j.expneurol.2016.07.023 [PubMed: 27477858]

Cholanian M, Wealing J, Levine RB, & Fregosi RF (2017). Developmental nicotine exposure alters potassium currents in hypoglossal motoneurons of neonatal rat. J Neurophysiol, 117(4), 1544–1552. doi:10.1152/jn.00774.2016 [PubMed: 28148643]

Clifford A, Lang L, & Chen R (2012). Effects of maternal cigarette smoking during pregnancy on cognitive parameters of children and young adults: a literature review. Neurotoxicol Teratol, 34(6), 560–570. doi:10.1016/j.ntt.2012.09.004 [PubMed: 23022448]

Coddou C, Bravo E, & Eugenin J (2009). Alterations in cholinergic sensitivity of respiratory neurons induced by pre-natal nicotine: a mechanism for respiratory dysfunction in neonatal mice. Philos Trans R Soc Lond B Biol Sci, 364(1529), 2527–2535. doi:10.1098/rstb.2009.0078 [PubMed: 19651654]

Consonni S, Leone S, Becchetti A, & Amadeo A (2009). Developmental and neurochemical features of cholinergic neurons in the murine cerebral cortex. BMC Neurosci, 10, 18. doi:10.1186/1471-2202-10-18 [PubMed: 19272148]

Contestabile A, Villani L, Fasolo A, Franzoni MF, Gribaudo L, Oktedalen O, & Fonnum F (1987). Topography of cholinergic and substance P pathways in the habenulo-interpeduncular system of the rat. An immunocytochemical and microchemical approach. Neuroscience, 21(1), 253–270. [PubMed: 2439945]

Daigle TL, Madisen L, Hage TA, Valley MT, Knoblich U, Larsen RS, … Zeng H (2018). A Suite of Transgenic Driver and Reporter Mouse Lines with Enhanced Brain-Cell-Type Targeting and Functionality. Cell, 174(2), 465–480 e422. doi:10.1016/j.cell.2018.06.035 [PubMed: 30007418]

Dwyer JB, McQuown SC, & Leslie FM (2009). The dynamic effects of nicotine on the developing brain. Pharmacol Ther, 122(2), 125–139. doi:10.1016/j.pharmthera.2009.02.003 [PubMed: 19268688]

El Mestikawy S, Wallen-Mackenzie A, Fortin GM, Descarries L, & Trudeau LE (2011). From glutamate co-release to vesicular synergy: vesicular glutamate transporters. Nat Rev Neurosci, 12(4), 204–216. doi:10.1038/nrn2969 [PubMed: 21415847]

Eugenin J, Otarola M, Bravo E, Coddou C, Cerpa V, Reyes-Parada M, … von Bernhardi R (2008). Prenatal to early postnatal nicotine exposure impairs central chemoreception and modifies breathing pattern in mouse neonates: a probable link to sudden infant death syndrome. J Neurosci, 28(51), 13907–13917. doi:10.1523/JNEUROSCI.4441-08.2008 [PubMed: 19091979]

Fedtsova N, & Turner E (1995). Brn-3.0 Expression identifies early post-mitotic CNS neurons and sensory neural precursors. Mechanisms of Development, 53, 291–304. [PubMed: 8645597]

Fiedler EP, Marks MJ, & Collins AC (1987). Postnatal development of cholinergic enzymes and receptors in mouse brain. J Neurochem, 49(3), 983–990. [PubMed: 3612135]

Frahm S, Antolin-Fontes B, Gorlich A, Zander JF, Ahnert-Hilger G, & Ibanez-Tallon I (2015). An essential role of acetylcholine-glutamate synergy at habenular synapses in nicotine dependence. Elife, 4, e11396. doi:10.7554/eLife.11396 [PubMed: 26623516]

Garcia AJ 3rd, Koschnitzky JE, & Ramirez JM (2013). The physiological determinants of sudden infant death syndrome. Respir Physiol Neurobiol, 189(2), 288–300. doi:10.1016/j.resp.2013.05.032 [PubMed: 23735486]

Gonzalez-Alzaga B, Lacasana M, Aguilar-Garduno C, Rodriguez-Barranco M, Ballester F, Rebagliato M, & Hernandez AF (2014). A systematic review of neurodevelopmental effects of prenatal and

postnatal organophosphate pesticide exposure. Toxicol Lett, 230(2), 104–121. doi:10.1016/j.toxlet.2013.11.019 [PubMed: 24291036]

Granger AJ, Mulder N, Saunders A, & Sabatini BL (2016). Cotransmission of acetylcholine and GABA. Neuropharmacology, 100, 40–46. doi:10.1016/j.neuropharm.2015.07.031 [PubMed: 26220313]

Granger AJ, Wallace ML, & Sabatini BL (2017). Multi-transmitter neurons in the mammalian central nervous system. Curr Opin Neurobiol, 45, 85–91. doi:10.1016/j.conb.2017.04.007 [PubMed: 28500992]

Gras C, Herzog E, Bellenchi GC, Bernard V, Ravassard P, Pohl M, … El Mestikawy S (2002). A third vesicular glutamate transporter expressed by cholinergic and serotoninergic neurons. J Neurosci, 22(13), 5442–5451. [PubMed: 12097496]

Gu Z, Lamb PW, & Yakel JL (2012). Cholinergic coordination of presynaptic and postsynaptic activity induces timing-dependent hippocampal synaptic plasticity. J Neurosci, 32(36), 12337–12348. doi:10.1523/JNEUROSCI.2129-12.2012 [PubMed: 22956824]

Gu Z, & Yakel JL (2011). Timing-dependent septal cholinergic induction of dynamic hippocampal synaptic plasticity. Neuron, 71(1), 155–165. doi:10.1016/j.neuron.2011.04.026 [PubMed: 21745645]

Gustavson K, Ystrom E, Stoltenberg C, Susser E, Suren P, Magnus P, … Reichborn-Kjennerud T (2017). Smoking in Pregnancy and Child ADHD. Pediatrics, 139(2). doi:10.1542/peds.2016-2509

Hakeem GF, Oddy L, Holcroft CA, & Abenhaim HA (2015). Incidence and determinants of sudden infant death syndrome: a population-based study on 37 million births. World J Pediatr, 11(1), 41–47. doi:10.1007/s12519-014-0530-9 [PubMed: 25447630]

Halff AW, Gomez-Varela D, John D, & Berg DK (2014). A novel mechanism for nicotinic potentiation of glutamatergic synapses. J Neurosci, 34(6), 2051–2064. doi:10.1523/JNEUROSCI.2795-13.2014 [PubMed: 24501347]

Hanse E, Seth H, & Riebe I (2013). AMPA-silent synapses in brain development and pathology. Nat Rev Neurosci, 14(12), 839–850. doi:10.1038/nrn3642 [PubMed: 24201185]

Haynes RL, Frelinger AL 3rd, Giles EK, Goldstein RD, Tran H, Kozakewich HP, … Michelson AD (2017). High serum serotonin in sudden infant death syndrome. Proc Natl Acad Sci U S A, 114(29), 7695–7700. doi:10.1073/pnas.1617374114 [PubMed: 28674018]

Hedrick T, Danskin B, Larsen RS, Ollerenshaw D, Groblewski P, Valley M, … Waters J (2016). Characterization of Channelrhodopsin and Archaerhodopsin in Cholinergic Neurons of Cre-Lox Transgenic Mice. PLoS One, 11(5), e0156596. doi:10.1371/journal.pone.0156596 [PubMed: 27243816]

Higley MJ, Gittis AH, Oldenburg IA, Balthasar N, Seal RP, Edwards RH, … Sabatini BL (2011). Cholinergic interneurons mediate fast VGluT3-dependent glutamatergic transmission in the striatum. PLoS One, 6(4), e19155. doi:10.1371/journal.pone.0019155 [PubMed: 21544206]

Hnasko TS, & Edwards RH (2012). Neurotransmitter corelease: mechanism and physiological role. Annu Rev Physiol, 74, 225–243. doi:10.1146/annurev-physiol-020911-153315 [PubMed: 22054239]

Hohmann CF, Pert CC, & Ebner FF (1985). Development of cholinergic markers in mouse forebrain. II. Muscarinic receptor binding in cortex. Brain Res, 355(2), 243–253. [PubMed: 4084779]

Horne RS, Franco P, Adamson TM, Groswasser J, & Kahn A (2002). Effects of body position on sleep and arousal characteristics in infants. Early Hum Dev, 69(1–2), 25–33. [PubMed: 12324180]

Horne RS, Franco P, Adamson TM, Groswasser J, & Kahn A (2004). Influences of maternal cigarette smoking on infant arousability. Early Hum Dev, 79(1), 49–58. doi:10.1016/j.earlhumdev.2004.04.005 [PubMed: 15282122]

Hsu YW, Tempest L, Quina LA, Wei AD, Zeng H, & Turner EE (2013). Medial habenula output circuit mediated by alpha5 nicotinic receptor-expressing GABAergic neurons in the interpeduncular nucleus. J Neurosci, 33(46), 18022–18035. doi:10.1523/JNEUROSCI.2927-13.2013 33/46/18022 [pii] [PubMed: 24227714]

Iwasaki K, Komiya H, Kakizaki M, Miyoshi C, Abe M, Sakimura K, … Yanagisawa M (2018). Ablation of Central Serotonergic Neurons Decreased REM Sleep and Attenuated Arousal Response. Front Neurosci, 12, 535. doi:10.3389/fnins.2018.00535 [PubMed: 30131671]

Jaarsma D, Ruigrok TJ, Caffe R, Cozzari C, Levey AI, Mugnaini E, & Voogd J (1997). Cholinergic innervation and receptors in the cerebellum. Prog Brain Res, 114, 67–96. [PubMed: 9193139]

Kahoud RJ, Elsen GE, Hevner RF, & Hodge RD (2014). Conditional ablation of Tbr2 results in abnormal development of the olfactory bulbs and subventricular zone-rostral migratory stream. Dev Dyn, 243(3), 440–450. doi:10.1002/dvdy.24090 [PubMed: 24550175]

Kang L, Tian MK, Bailey CD, & Lambe EK (2015). Dendritic spine density of prefrontal layer 6 pyramidal neurons in relation to apical dendrite sculpting by nicotinic acetylcholine receptors. Front Cell Neurosci, 9, 398. doi:10.3389/fncel.2015.00398 [PubMed: 26500498]

Kataoka K, Nakamura Y, & Hassler R (1973). Habenulo-interpeduncular tract: a possible cholinergic neuron in rat brain. Brain Res, 62(1), 264–267. [PubMed: 4765115]

Kaur S, Pedersen NP, Yokota S, Hur EE, Fuller PM, Lazarus M, … Saper CB (2013). Glutamatergic signaling from the parabrachial nucleus plays a critical role in hypercapnic arousal. J Neurosci, 33(18), 7627–7640. doi:10.1523/JNEUROSCI.0173-13.2013 [PubMed: 23637157]

Kaur S, Wang JL, Ferrari L, Thankachan S, Kroeger D, Venner A, … Saper CB (2017). A Genetically Defined Circuit for Arousal from Sleep during Hypercapnia. Neuron, 96(5), 1153–1167 e1155. doi:10.1016/j.neuron.2017.10.009 [PubMed: 29103805]

Kawa K (2002). Acute synaptic modulation by nicotinic agonists in developing cerebellar Purkinje cells of the rat. J Physiol, 538(Pt 1), 87–102. [PubMed: 11773319]

Kinney HC, Richerson GB, Dymecki SM, Darnall RA, & Nattie EE (2009). The brainstem and serotonin in the sudden infant death syndrome. Annu Rev Pathol, 4, 517–550. doi:10.1146/annurev.pathol.4.110807.092322 [PubMed: 19400695]

Lein ES, Hawrylycz MJ, Ao N, Ayres M, Bensinger A, Bernard A, … Jones AR (2007). Genome-wide atlas of gene expression in the adult mouse brain. Nature, 445(7124), 168–176. doi:nature05453 [pii] 10.1038/nature05453 [PubMed: 17151600]

Li X, Yu B, Sun Q, Zhang Y, Ren M, Zhang X, … Qiu Z (2018). Generation of a whole-brain atlas for the cholinergic system and mesoscopic projectome analysis of basal forebrain cholinergic neurons. Proc Natl Acad Sci U S A, 115(2), 415–420. doi:10.1073/pnas.1703601115 [PubMed: 29259118]

Liang K, Poytress BS, Chen Y, Leslie FM, Weinberger NM, & Metherate R (2006). Neonatal nicotine exposure impairs nicotinic enhancement of central auditory processing and auditory learning in adult rats. Eur J Neurosci, 24(3), 857–866. doi:10.1111/j.1460-9568.2006.04945.x [PubMed: 16848798]

Lindblad F, & Hjern A (2010). ADHD after fetal exposure to maternal smoking. Nicotine Tob Res, 12(4), 408–415. doi:10.1093/ntr/ntq017 [PubMed: 20176681]

Linnet KM, Dalsgaard S, Obel C, Wisborg K, Henriksen TB, Rodriguez A, … Jarvelin MR (2003). Maternal lifestyle factors in pregnancy risk of attention deficit hyperactivity disorder and associated behaviors: review of the current evidence. Am J Psychiatry, 160(6), 1028–1040. doi:10.1176/appi.ajp.160.6.1028 [PubMed: 12777257]

Lozada AF, Wang X, Gounko NV, Massey KA, Duan J, Liu Z, & Berg DK (2012a). Glutamatergic synapse formation is promoted by alpha7-containing nicotinic acetylcholine receptors. J Neurosci, 32(22), 7651–7661. doi:10.1523/JNEUROSCI.6246-11.2012 [PubMed: 22649244]

Lozada AF, Wang X, Gounko NV, Massey KA, Duan J, Liu Z, & Berg DK (2012b). Induction of dendritic spines by beta2-containing nicotinic receptors. J Neurosci, 32(24), 8391–8400. doi:10.1523/JNEUROSCI.6247-11.2012 [PubMed: 22699919]

Luquin E, Huerta I, Aymerich MS, & Mengual E (2018). Stereological Estimates of Glutamatergic, GABAergic, and Cholinergic Neurons in the Pedunculopontine and Laterodorsal Tegmental Nuclei in the Rat. Front Neuroanat, 12, 34. doi:10.3389/fnana.2018.00034 [PubMed: 29867374]

Madisen L, Garner AR, Shimaoka D, Chuong AS, Klapoetke NC, Li L, … Zeng H (2015). Transgenic mice for intersectional targeting of neural sensors and effectors with high specificity and performance. Neuron, 85(5), 942–958. doi:10.1016/j.neuron.2015.02.022 [PubMed: 25741722]

Madisen L, Zwingman TA, Sunkin SM, Oh SW, Zariwala HA, Gu H, … Zeng H (2010). A robust and high-throughput Cre reporting and characterization system for the whole mouse brain. Nat Neurosci, 13(1), 133–140. doi:nn.2467 [pii] 10.1038/nn.2467 [PubMed: 20023653]

Mateika JH, Komnenov D, Pop A, & Kuhn DM (2018). Genetic depletion of 5HT increases central apnea frequency and duration and dampens arousal but does not impact the circadian modulation of these variables. J Appl Physiol (1985). doi:10.1152/japplphysiol.00724.2018

Mentis GZ, Alvarez FJ, Bonnot A, Richards DS, Gonzalez-Forero D, Zerda R, & O'Donovan MJ (2005). Noncholinergic excitatory actions of motoneurons in the neonatal mammalian spinal cord. Proc Natl Acad Sci U S A, 102(20), 7344–7349. doi:10.1073/pnas.0502788102 [PubMed: 15883359]

Mihalas AB, & Hevner RF (2017). Control of Neuronal Development by T-Box Genes in the Brain. Curr Top Dev Biol, 122, 279–312. doi:10.1016/bs.ctdb.2016.08.001 [PubMed: 28057268]

Mufson EJ, Martin TL, Mash DC, Wainer BH, & Mesulam MM (1986). Cholinergic projections from the parabigeminal nucleus (Ch8) to the superior colliculus in the mouse: a combined analysis of horseradish peroxidase transport and choline acetyltransferase immunohistochemistry. Brain Res, 370(1), 144–148. [PubMed: 3708316]

Nishimaru H, Restrepo CE, Ryge J, Yanagawa Y, & Kiehn O (2005). Mammalian motor neurons corelease glutamate and acetylcholine at central synapses. Proc Natl Acad Sci U S A, 102(14), 5245–5249. doi:10.1073/pnas.0501331102 [PubMed: 15781854]

Paez-Gonzalez P, Asrican B, Rodriguez E, & Kuo CT (2014). Identification of distinct ChAT(+) neurons and activity-dependent control of postnatal SVZ neurogenesis. Nat Neurosci, 17(7), 934–942. doi:10.1038/nn.3734 [PubMed: 24880216]

Palmiter RD (2018). The Parabrachial Nucleus: CGRP Neurons Function as a General Alarm. Trends Neurosci, 41(5), 280–293. doi:10.1016/j.tins.2018.03.007 [PubMed: 29703377]

Paxinos G, & Franklin KBJ (2001). The mouse brain in stereotaxic coordinates (2nd ed.). San Diego, Calif. London: Academic.

Picciotto MR, Higley MJ, & Mineur YS (2012). Acetylcholine as a neuromodulator: cholinergic signaling shapes nervous system function and behavior. Neuron, 76(1), 116–129. doi:10.1016/j.neuron.2012.08.036 S0896–6273(12)00802–1 [pii] [PubMed: 23040810]

Powell GL, Levine RB, Frazier AM, & Fregosi RF (2015). Influence of developmental nicotine exposure on spike-timing precision and reliability in hypoglossal motoneurons. J Neurophysiol, 113(6), 1862–1872. doi:10.1152/jn.00838.2014 [PubMed: 25552642]

Qin C, & Luo M (2009). Neurochemical phenotypes of the afferent and efferent projections of the mouse medial habenula. Neuroscience. doi:S0306–4522(09)00544–2 [pii] 10.1016/j.neuroscience.2009.03.085

Quina LA, Harris J, Zeng H, & Turner EE (2017). Specific connections of the interpeduncular subnuclei reveal distinct components of the habenulopeduncular pathway. J Comp Neurol, 525(12), 2632–2656. doi:10.1002/cne.24221 [PubMed: 28387937]

Quina LA, Pak W, Lanier J, Banwait P, Gratwick K, Liu Y, … Turner EE (2005). Brn3a-expressing retinal ganglion cells project specifically to thalamocortical and collicular visual pathways. J Neurosci, 25(50), 11595–11604. doi:25/50/11595 [pii] 10.1523/JNEUROSCI.2837-05.2005 [PubMed: 16354917]

Ramirez JM, Folkow LP, & Blix AS (2007). Hypoxia tolerance in mammals and birds: from the wilderness to the clinic. Annu Rev Physiol, 69, 113–143. doi:10.1146/annurev.physiol.69.031905.163111 [PubMed: 17037981]

Ramirez S, Allen T, Villagracia L, Chae Y, Ramirez JM, & Rubens DD (2016). Inner ear lesion and the differential roles of hypoxia and hypercarbia in triggering active movements: Potential implication for the Sudden Infant Death Syndrome. Neuroscience, 337, 9–16. doi:10.1016/j.neuroscience.2016.08.054 [PubMed: 27634772]

Rathouz MM, Vijayaraghavan S, & Berg DK (1995). Acetylcholine differentially affects intracellular calcium via nicotinic and muscarinic receptors on the same population of neurons. J Biol Chem, 270(24), 14366–14375. [PubMed: 7782297]

Ray RS, Corcoran AE, Brust RD, Kim JC, Richerson GB, Nattie E, & Dymecki SM (2011). Impaired respiratory and body temperature control upon acute serotonergic neuron inhibition. Science, 333(6042), 637–642. doi:10.1126/science.1205295 [PubMed: 21798952]

Ren J, Qin C, Hu F, Tan J, Qiu L, Zhao S, … Luo M (2011). Habenula "cholinergic" neurons co-release glutamate and acetylcholine and activate postsynaptic neurons via distinct transmission

modes. Neuron, 69(3), 445–452. doi:S0896–6273(10)01088–3 [pii] 10.1016/j.neuron.2010.12.038 [PubMed: 21315256]

Roerig B, Nelson DA, & Katz LC (1997). Fast synaptic signaling by nicotinic acetylcholine and serotonin 5-HT3 receptors in developing visual cortex. J Neurosci, 17(21), 8353–8362. [PubMed: 9334409]

Rossi J, Balthasar N, Olson D, Scott M, Berglund E, Lee CE, … Elmquist JK (2011). Melanocortin-4 receptors expressed by cholinergic neurons regulate energy balance and glucose homeostasis. Cell Metab, 13(2), 195–204. doi:S1550–4131(11)00011–8 [pii] 10.1016/j.cmet.2011.01.010 [PubMed: 21284986]

Rumpel S, Kattenstroth G, & Gottmann K (2004). Silent synapses in the immature visual cortex: layer-specific developmental regulation. J Neurophysiol, 91(2), 1097–1101. doi:10.1152/jn.00443.2003 [PubMed: 14762153]

Saunders A, Granger AJ, & Sabatini BL (2015). Corelease of acetylcholine and GABA from cholinergic forebrain neurons. Elife, 4. doi:10.7554/eLife.06412

Shao XM, & Feldman JL (2009). Central cholinergic regulation of respiration: nicotinic receptors. Acta Pharmacol Sin, 30(6), 761–770. doi:10.1038/aps.2009.88 [PubMed: 19498418]

Soria-Gomez E, Busquets-Garcia A, Hu F, Mehidi A, Cannich A, Roux L, … Marsicano G (2015). Habenular CB1 Receptors Control the Expression of Aversive Memories. Neuron, 88(2), 306–313. doi:10.1016/j.neuron.2015.08.035 [PubMed: 26412490]

Stornetta RL, Macon CJ, Nguyen TM, Coates MB, & Guyenet PG (2013). Cholinergic neurons in the mouse rostral ventrolateral medulla target sensory afferent areas. Brain Struct Funct, 218(2), 455–475. doi:10.1007/s00429-012-0408-3 [PubMed: 22460939]

Takacs VT, Cserep C, Schlingloff D, Posfai B, Szonyi A, Sos KE, … Nyiri G (2018). Co-transmission of acetylcholine and GABA regulates hippocampal states. Nat Commun, 9(1), 2848. doi:10.1038/s41467-018-05136-1 [PubMed: 30030438]

Thiele A (2013). Muscarinic signaling in the brain. Annu Rev Neurosci, 36, 271–294. doi:10.1146/annurev-neuro-062012-170433 [PubMed: 23841840]

Thompson CL, Ng L, Menon V, Martinez S, Lee CK, Glattfelder K, … Jones AR (2014). A high-resolution spatiotemporal atlas of gene expression of the developing mouse brain. Neuron, 83(2), 309–323. doi:10.1016/j.neuron.2014.05.033 [PubMed: 24952961]

Tiesler CM, & Heinrich J (2014). Prenatal nicotine exposure and child behavioural problems. Eur Child Adolesc Psychiatry, 23(10), 913–929. doi:10.1007/s00787-014-0615-y [PubMed: 25241028]

Trudeau LE, Hnasko TS, Wallen-Mackenzie A, Morales M, Rayport S, & Sulzer D (2014). The multilingual nature of dopamine neurons. Prog Brain Res, 211, 141–164. doi:10.1016/B978-0-444-63425-2.00006-4 [PubMed: 24968779]

Tryba AK, Pena F, & Ramirez JM (2006). Gasping activity in vitro: a rhythm dependent on 5-HT2A receptors. J Neurosci, 26(10), 2623–2634. doi:10.1523/JNEUROSCI.4186-05.2006 [PubMed: 16525041]

Vivekanandarajah A, Waters KA, & Machaalani R (2019). Cigarette smoke exposure effects on the brainstem expression of nicotinic acetylcholine receptors (nAChRs), and on cardiac, respiratory and sleep physiologies. Respir Physiol Neurobiol, 259, 1–15. doi:10.1016/j.resp.2018.07.007 [PubMed: 30031221]

von Engelhardt J, Eliava M, Meyer AH, Rozov A, & Monyer H (2007). Functional characterization of intrinsic cholinergic interneurons in the cortex. J Neurosci, 27(21), 5633–5642. doi:10.1523/JNEUROSCI.4647-06.2007 [PubMed: 17522308]

Wang HL, & Morales M (2009). Pedunculopontine and laterodorsal tegmental nuclei contain distinct populations of cholinergic, glutamatergic and GABAergic neurons in the rat. Eur J Neurosci, 29(2), 340–358. doi:10.1111/j.1460-9568.2008.06576.x [PubMed: 19200238]

Wollman LB, Levine RB, & Fregosi RF (2018). Developmental nicotine exposure alters glycinergic neurotransmission to hypoglossal motoneurons in neonatal rats. J Neurophysiol, 120(3), 1135–1142. doi:10.1152/jn.00600.2017 [PubMed: 29847237]

Woolf NJ (1991). Cholinergic systems in mammalian brain and spinal cord. Prog Neurobiol, 37(6), 475–524. [PubMed: 1763188]

Wu H, Williams J, & Nathans J (2014). Complete morphologies of basal forebrain cholinergic neurons in the mouse. Elife, 3, e02444. doi:10.7554/eLife.02444 [PubMed: 24894464]

Xiao MY, Wasling P, Hanse E, & Gustafsson B (2004). Creation of AMPA-silent synapses in the neonatal hippocampus. Nat Neurosci, 7(3), 236–243. doi:10.1038/nn1196 [PubMed: 14966524]

Yokota S, Kaur S, VanderHorst VG, Saper CB, & Chamberlin NL (2015). Respiratory-related outputs of glutamatergic, hypercapnia-responsive parabrachial neurons in mice. J Comp Neurol, 523(6), 907–920. doi:10.1002/cne.23720 [PubMed: 25424719]

Zhang K, & Wang X (2013). Maternal smoking and increased risk of sudden infant death syndrome: a meta-analysis. Leg Med (Tokyo), 15(3), 115–121. doi:10.1016/j.legalmed.2012.10.007 [PubMed: 23219585]

Zhang X, Liu C, Miao H, Gong ZH, & Nordberg A (1998). Postnatal changes of nicotinic acetylcholine receptor alpha 2, alpha 3, alpha 4, alpha 7 and beta 2 subunits genes expression in rat brain. Int J Dev Neurosci, 16(6), 507–518. [PubMed: 9881299]

Zhang Y, Hamilton SE, Nathanson NM, & Yan J (2006). Decreased input-specific plasticity of the auditory cortex in mice lacking M1 muscarinic acetylcholine receptors. Cereb Cortex, 16(9), 1258–1265. doi:10.1093/cercor/bhj067 [PubMed: 16292003]

Zhang Y, Kaneko R, Yanagawa Y, & Saito Y (2014). The vestibulo- and preposito-cerebellar cholinergic neurons of a ChAT-tdTomato transgenic rat exhibit heterogeneous firing properties and the expression of various neurotransmitter receptors. Eur J Neurosci, 39(8), 1294–1313. doi: 10.1111/ejn.12509 [PubMed: 24593297]

Zoli M, Le Novere N, Hill JA Jr., & Changeux JP (1995). Developmental regulation of nicotinic ACh receptor subunit mRNAs in the rat central and peripheral nervous systems. J Neurosci, 15(3 Pt 1), 1912–1939. [PubMed: 7891142]

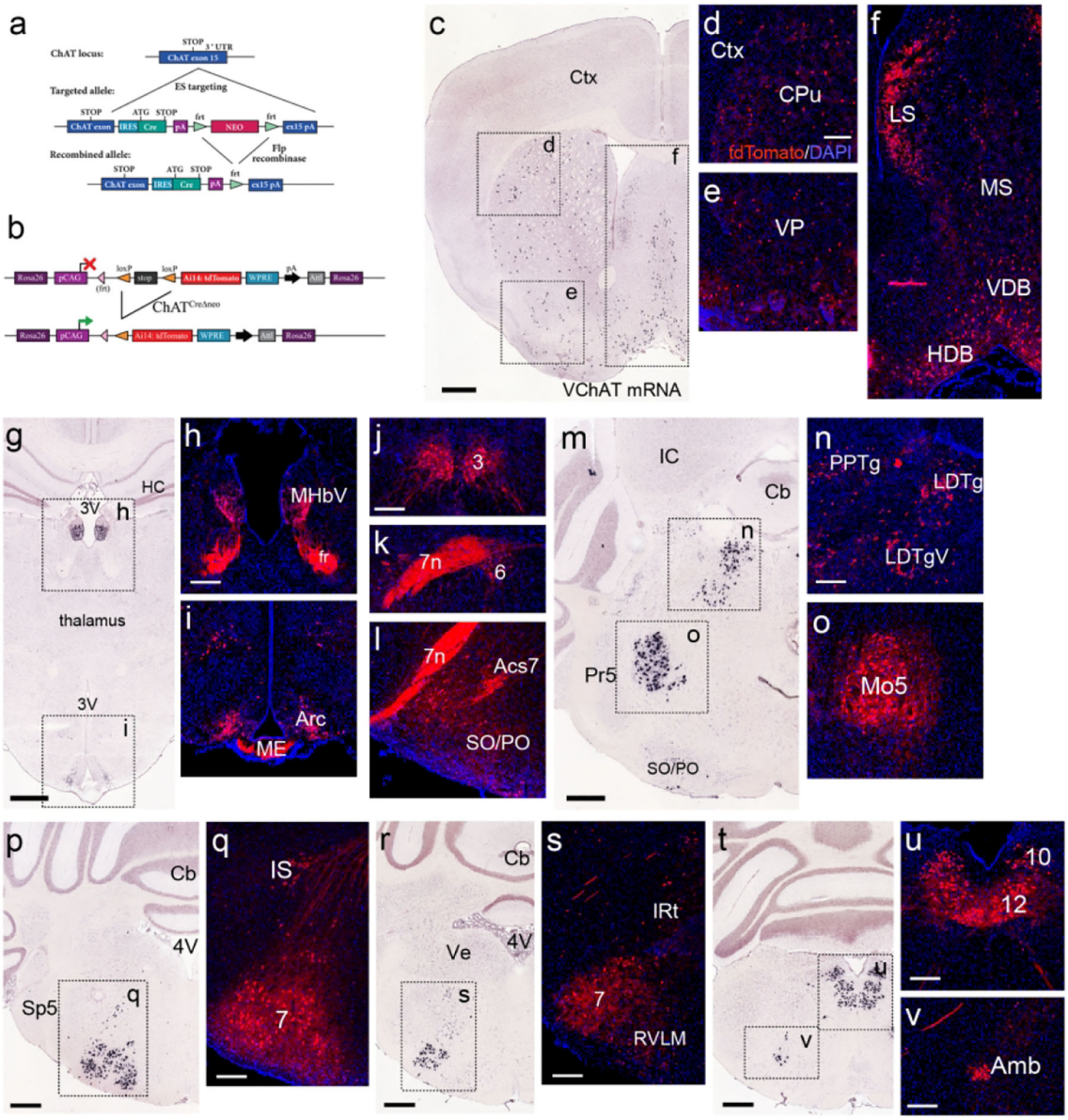

Figure 1. Chat^{Cre}-mediated recombination marks known cholinergic neurons throughout the CNS.

At each axial level, VChAT mRNA expression from the Allen Brain Atlas is used as an independent marker of the cholinergic phenotype and compared to Chat^{Cre}-induced tdT expression. **(a,b)** Transgenic strategy for cre-mediated marking of cholinergic neurons. (a) Flp recombinase was used to excise neomycin resistance cassette from a widely used cre driver in order to eliminate ectopic expression noted when using the parent transgenic line. (b) Chat^{Cre} was used to remove a loxP-stop-loxP cassette in the Ai14 reporter allele to activate tdT expression. **(c–f)** Cholinergic markers in the striatum and septum. **(g–i)** Cholinergic markers in the habenula and hypothalamus. **(j)** TdT expression in the oculomotor (3) nucleus. **(k)** TdT expression in the facial nerve and abducens (6) nucleus. **(l)** TdT expression in the facial nerve, accessory facial nucleus, and superior olive/periolivary

region. **(m–o)** Cholinergic markers in the mesopontine region, including the pedunculopontine tegmental nucleus, laterodorsal tegmental nucleus and motor nucleus of the trigeminal nerve. **(p–q**) Cholinergic markers in the rostral medulla. **(r–s)** Cholinergic markers in the medulla; the intermediate and rostroventrolateral reticular areas contain ChAT-expressing neurons which may be involved in regulation of respiratory rhythms. **(t–v)** Cholinergic markers in the vagal and hypoglossal motor nuclei and nucleus ambiguus. Legend: 3, oculomotor nucleus; 3V, third ventricle; 4V, fourth ventricle; 6, abducens nucleus; 7, facial nucleus; 7n, facial nerve; 10, motor nucleus of the vagus nerve; 12, motor nucleus of the hypoglossal nerve; Acs7, accessory facial nucleus; Amb, nucleus ambiguus; Arc, arcuate nucleus; Cb, cerebellum; CPu, caudate/putamen; Ctx, neocortex; HC, hippocampus; HDB, horizontal limb, diagonal band; fr, fasciculus retroflexus; IC, inferior colliculus; IRt, intermediate reticular nucleus; IS, inferior salivatory (autonomic) nucleus; LDTg, laterodorsal tegmental nucleus (D, dorsal, V, ventral part); LS, lateral septum; ME, median eminence; MHbV, medial habenula, ventral part; Mo5, motor nucleus of trigeminal nerve; MS, medial septum; PO, periolivary nucleus; Pr5, principal sensory trigeminal nucleus; PPTg, pedunculopontine tegmental nucleus; RVLM, rostroventrolateral medulla; SO, superior olive; Sp5, spinal trigeminal sensory nucleus; VDB, vertical limb, diagonal band; Ve, vestibular area; VP, ventral pallidum. Scale c,g,m,p,r,t: 500μm; all fluorescence views: 200μm.

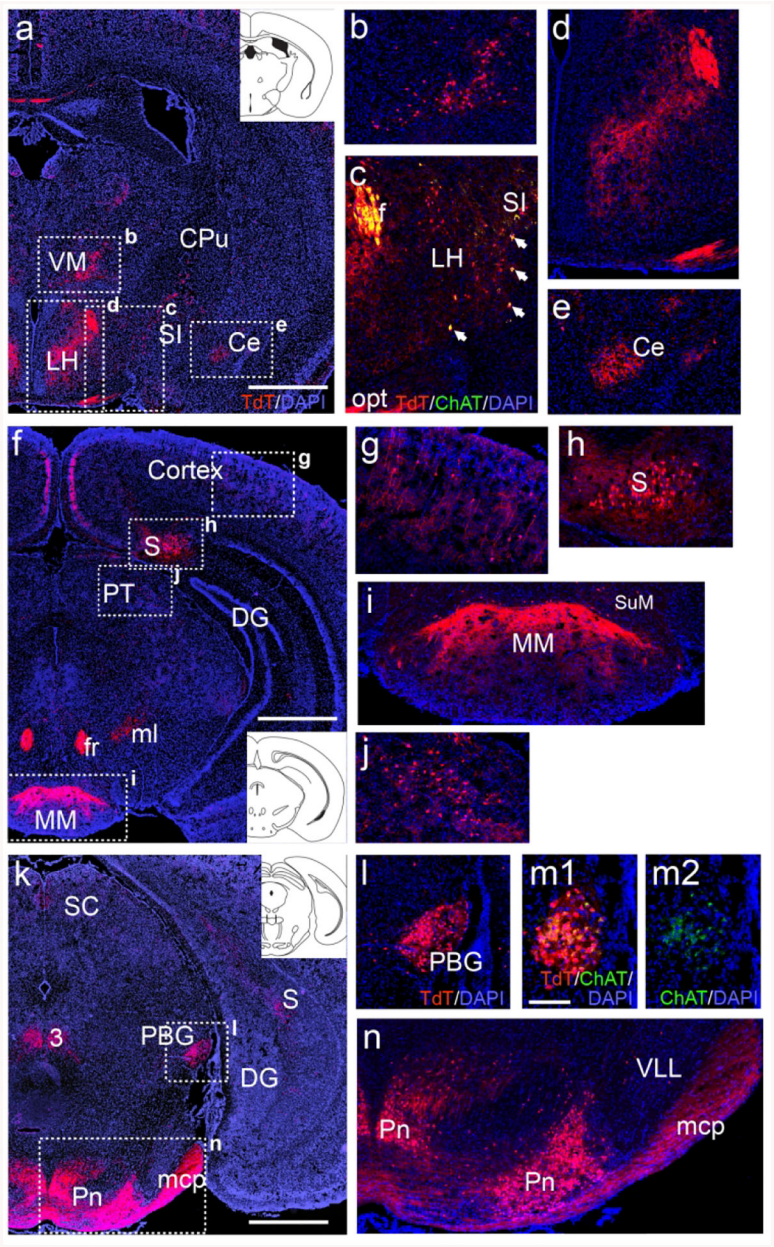

Figure 2. Chat^{tdT} expression in telencephalic, diencephalic, and mesopontine neurons not widely recognized as cholinergic.

(a–e) Expression of tdT fluorescence in the thalamus, hypothalamus, and amygdala of Chat^{tdT} mice. A coronal section is shown, corresponding to bregma −0.94 in a standard atlas (inset in A, Paxinos & Franklin, 2001) (b) Expression of tdT in cell bodies of the ventromedial thalamus. (c) Expression of tdT in the rostral part of the LH and adjacent SI, from a section adjacent to that shown in (a), also stained with anti-ChAT antisera. Cell bodies in the LH express tdT but no longer express detectable levels of ChAT protein, while cell bodies in the SI express both markers (arrows), consistent with other striatal cholinergic neurons. The optic tract (from retina) and fornix (from subiculum) are also labeled. In (d,e) fiber terminals appear in LH and Ce (from parabrachial nucleus). **(f–j)** Expression of Chat^{tdT}

in the neocortex, hippocampus (subiculum) and pretectum (atlas level bregma −2.92, inset). Fiber tracts in (f) include fr (from medial habenula), and ml (from cuneate/gracile nuclei). (g) Detail of small non-pyramidal neurons that appear throughout the cortex. (h) TdT expression in cell bodies in the subiculum. (i) Fibers from the subiculum terminating in MM; a few cell bodies can be seen in SuM. (j) Detail of cell bodies in the pretectum. **(k–n)** TdT expression in the midbrain and pontine nucleus (atlas level bregma −4.24, inset). The fiber tract mcp is also seen (from pons). (l) Detail of tdT expression in PBG. (m1, m2) TdT expression and ChAT immunoreactivity in an adjacent section through PBG, showing that faint expression of ChAT protein can be detected in the adult nucleus. (n) TdT expression in the pontine gray and its efferent tract mcp. Expression is restricted to the most medial and most lateral parts of the pontine nucleus. Legend: 3, oculomotor nucleus; Ce, central amygdala; CPu, caudate/putamen; DG, dentate gyrus; f, fornix; fr, fasciculus retroflexus; LH, lateral hypothalamus; mcp, middle cerebellar peduncle; ml, medial lemniscus; MM, medial mammillary nucleus; opt, optic tract; PBG, parabigeminal nucleus; Pn, pontine nucleus; PT, pretectum; S, subiculum; SC, superior colliculus; SI, substantia innominata; SuM, supramammillary nucleus; VLL, ventral nucleus of lateral lemniscus; VM, ventromedial nucleus of thalamus. Scale a,f,k: 1mm; m: 100μm.

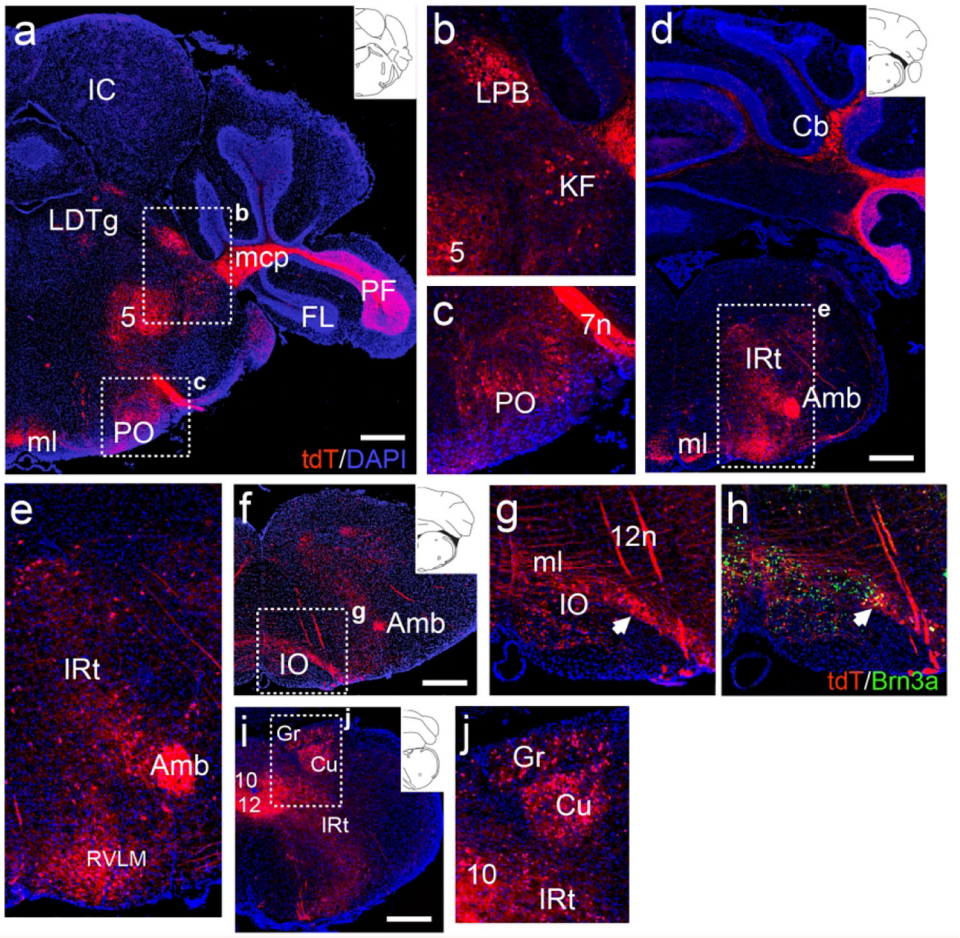

Figure 3. Chat^{tdT} expression in brainstem neurons not known to be cholinergic.

(a–c) Expression of Chat^{tdT} in the caudal pons (atlas level bregma −5.34, inset). Labeled cells are seen in the parabrachial complex and periolivary region. Fiber tracts can be seen in the mcp (from pontine nucleus) and ml (from cuneate/gracile nuclei). (b) Detail of expression in LPB and KF of the parabrachial complex. (c) Detail of expression in PO. **(d,e)** Expression of tdT in the rostral medulla, at the rostral end of the nucleus ambiguus (atlas level bregma −6.64, inset). Cell bodies are observed in IRt and RVLM. **(f,g)** Expression of tdT in the medulla, near the caudal end of the nucleus ambiguus. Cell bodies are observed in the lateral part of IO. Transverse fiber tracts are forming the ml (atlas level bregma −6.84, inset). **(h)** Section adjacent to (g) immunostained for the transcription factor Brn3a, identifying IO neurons. **(i,j)** Expression of tdT in the caudal medulla, (atlas level bregma −7.92, inset). (j) Detail of expression in the gracile/cuneate nuclei. Legend: 5, motor nucleus of trigeminal nerve; 7n, facial nerve; 10, motor nucleus of the vagus nerve; 12, motor nucleus of the hypoglossal nerve (12n); Amb, nucleus ambiguus; Cb, cerebellum; Cu, cuneate nucleus; FL, flocculus; Gr, gracile nucleus; IC, inferior colliculus; IO, inferior olive; IRt, intermediate reticular area (of medulla); KF, Kölliker-Fuse nucleus; LDTg, laterodorsal tegmental nucleus; LPB, lateral parabrachial nucleus; mcp, middle cerebellar peduncle; ml, medial lemniscus; PF, parafloccullus; PO, periolivary nucleus; RVLM, rostroventrolateral medulla. All sections are counterstained with DAPI (blue). Scale: a, d, f, i: 500μm.

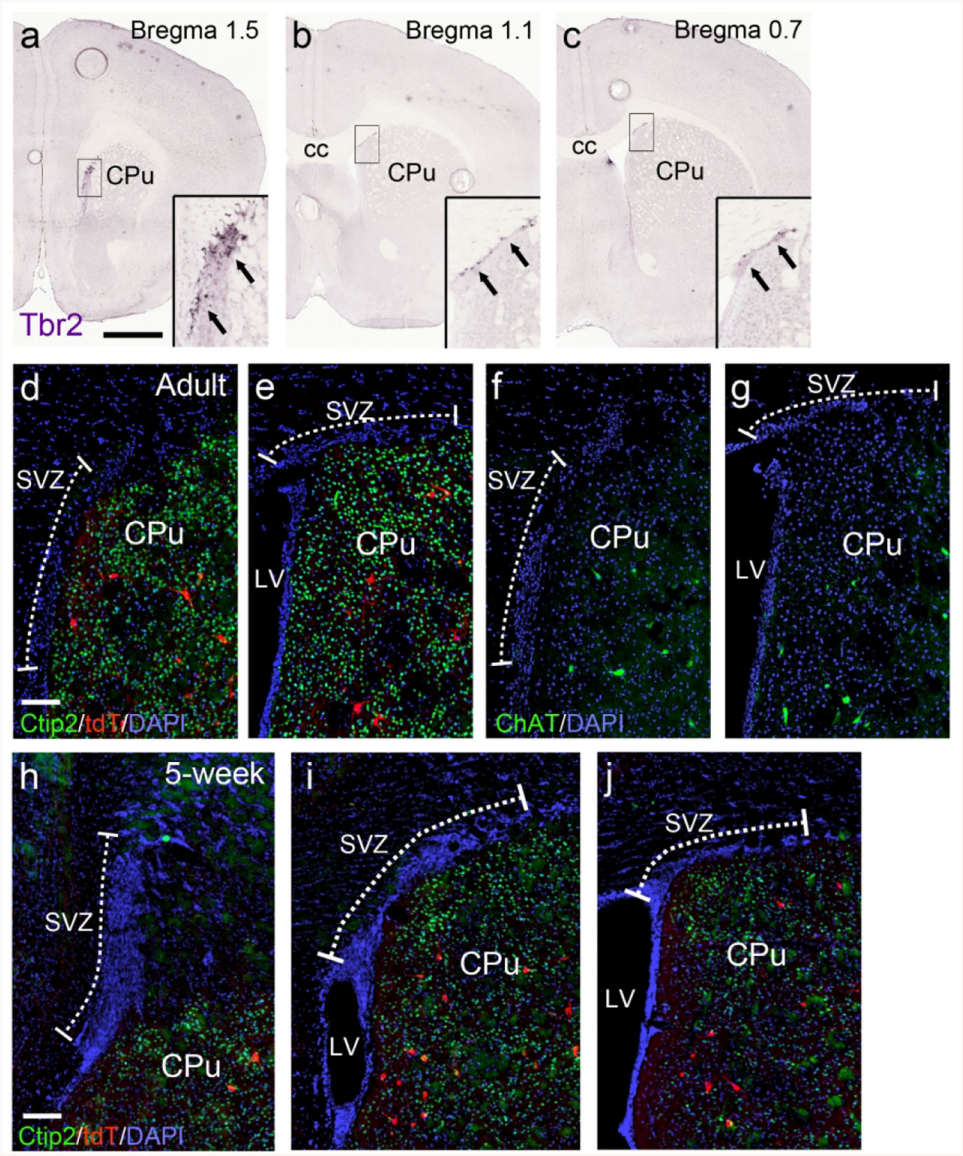

Figure 4. Chat^{tdT} neurons are absent from the subventricular zone.

Mice were examined at age 5 weeks and 5 months for the expression of Chat^{tdT} and ChAT immunoreactivity in the SVZ. **(a–c)** Expression of Tbr2 mRNA in the adult mouse subventricular zone at rostral, central, and caudal levels of the SVZ (Allen Brain Atlas), defining the VZ neurogenic area. **(d,e)** Expression of Chat^{tdT} in the 5-month old adult mouse brain at bregma 1.3 (d) and bregma 1.0 (e). Expression of the nuclear factor Ctip2 in medium spiny neurons defines the caudate/putamen compartment. Intrinsic cholinergic neurons are confined to the striatal compartment. No tdT-expressing neurons are observed in the SVZ (brackets). **(f,g)** Immunofluorescence for ChAT protein expression in sections adjacent to those shown in (d,e). **(h–j)** Expression of Chat^{tdT} in the 5-week old (P37) adolescent mouse brain at levels corresponding to bregma 1.7 (h), 1.4 (i), and 1.0 (j) in the adult brain. Legend: cc, corpus callosum; CPu, caudate/putamen; LV, lateral ventricle; SVZ,

subventricular zone. The approximate extent of the SVZ is designated by a dashed line. Scale: a–c, 1mm; d–g, h–j, 100μm.

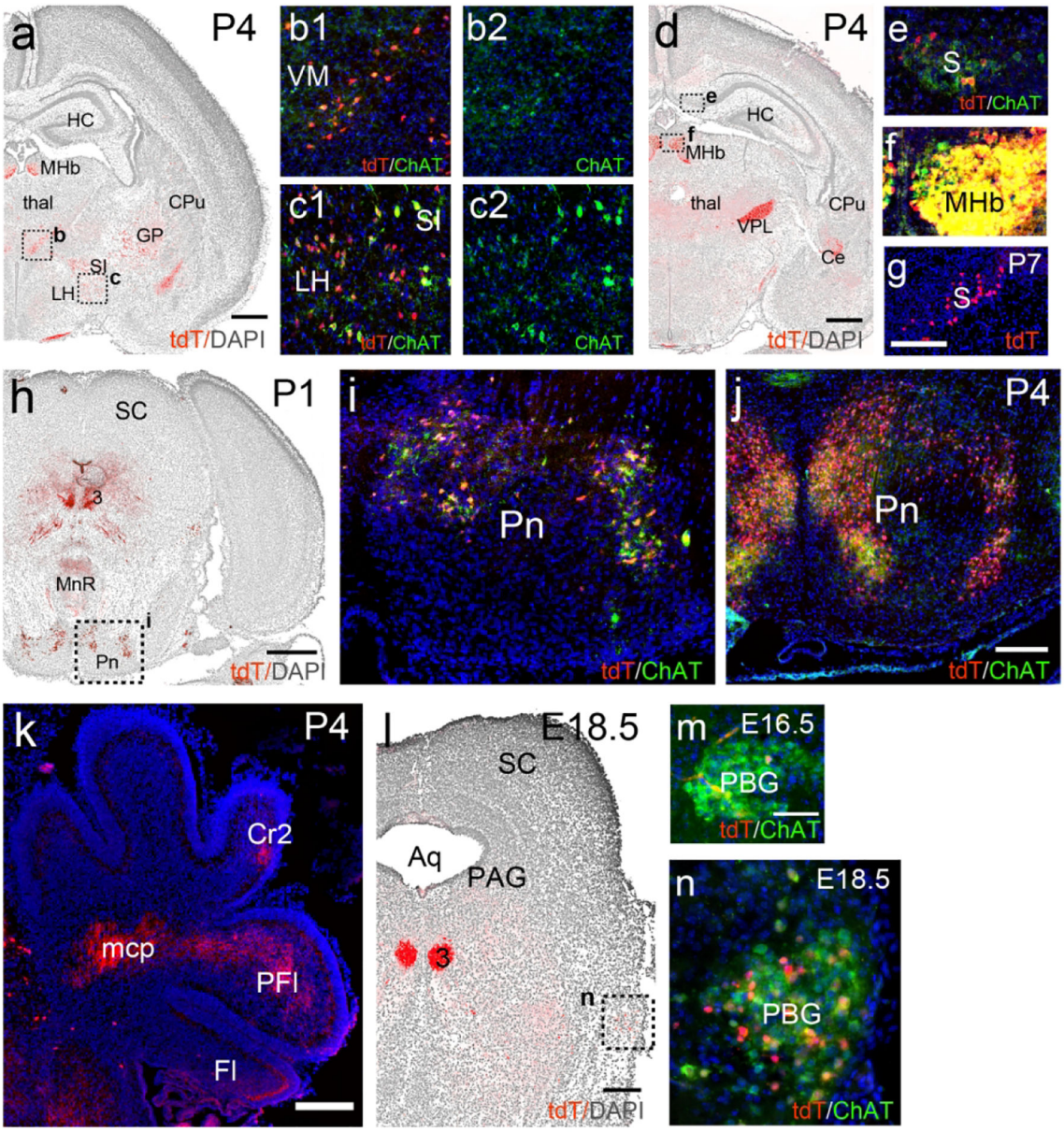

Figure 5. Developmental time course of Chat^{tdT} reporter expression and ChAT immunoreactivity in the subiculum, thalamus, pontocerebellar system and parabigeminal nucleus.

Chat^{tdT} mice were analyzed for tdT expression and ChAT immunofluorescence at E16.5, E18.5, P1, P4, and P7. In low-power images the nuclear staining for DAPI appears as a gray reverse image to show the underlying anatomical structures. **(a–c)** Expression in the diencephalon and striatum at P4. **(d–f)** Expression in the subiculum and diencephalon at P4. Fiber terminals in (d) are evident in VPL and Ce. Weak but detectable ChAT protein expression is co-localized with tdT in the subiculum (e). In (f) the MHb is imaged with the same exposure parameters as the subiculum in (e) to allow semi-quantitative comparison of ChAT expression. **(g)** Expression of tdT in the subiculum at P7. **(h,i)** Expression in the mesopontine region at P1. **(j,k)** Expression in the pontine nucleus (j) and labeled mossy fiber

projections in the cerebellum (k) at P4. **(l–n)** Expression in PBG. Chat^{tdT} and ChAT immunoreactivity are first detected in a few cells at E16.5 (m), and colocalization is robust by E18.5 (l,n). Legend: 3, oculomotor nucleus; Aq, aqueduct; Ce, central amygdala; CPu, caudate/putamen; Cr2, Crus2 (of cerebellum); Fl, flocculus; GP, globus pallidus; HC, hippocampus; LH, lateral hypothalamus; mcp, middle cerebellar peduncle; MHb, medial habenula; MnR, median raphe; PAG, periaqueductal gray; PBG, parabigeminal nucleus; PFl, paraflocculus; Pn, pontine nucleus; S, subiculum; SC, superior colliculus; SI, substantia innominata; thal, thalamus; VM, ventromedial thalamic nucleus;; VPL, ventral posterolateral thalamic nucleus. Scale: a,d,h,k, 500μm; g,j, 200μm; m, 50μm.

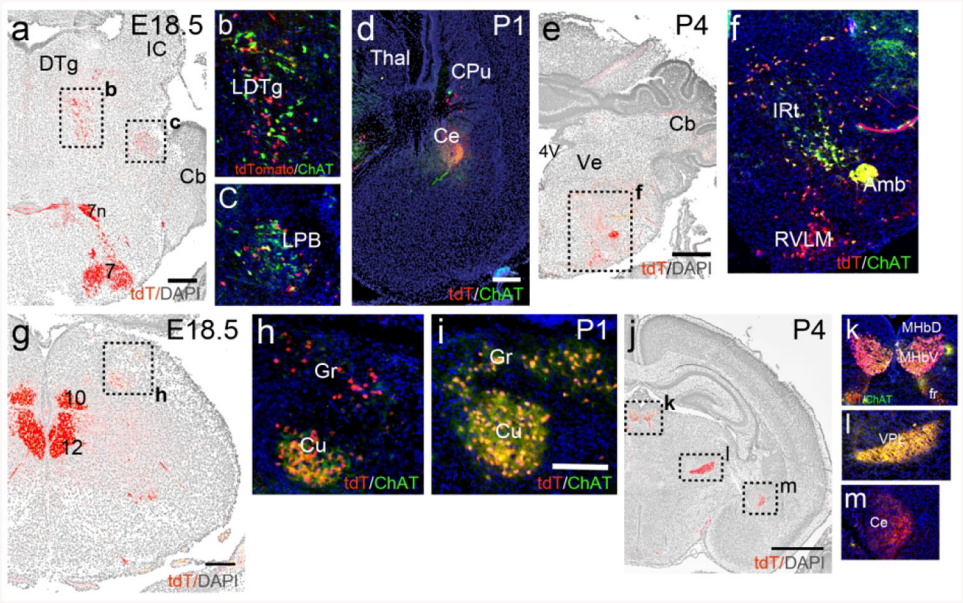

Figure 6. Developmental time course of Chat^{tdT} expression in neurons of the mesopontine tegmentum and medulla and their efferent fibers.

Chat^{tdT} mice were analyzed for tdT expression and ChAT immunofluorescence at E18.5, P1, P4. Nuclear staining for DAPI appears as a gray reverse image to show the underlying anatomical structures. **(a–c)** Expression in the LDTg and LPB in E18.5. **(d)** Chat^{tdT}/ChAT immunoreactive fibers originating in LPB are evident in Ce by P1. **(e,f)** Expression in the rostral medulla at P4. **(g,h)** Expression in the caudal medulla at E18.5. **(i)** Expression in the cuneate and gracile nuclei at P1. **(j–m)** Chat^{tdT} fiber projections in the thalamus and amygdala at P4. (k) Shows expression in the MHb and efferents in fasciculus retroflexus. (l) Shows fiber expression in the VPL originating in the gracilis/cuneate nuclei. (m) Fiber expression in Ce, originating in the LPB. ChAT immunoreactivity is diminished by this stage. Legend: 4V, fourth ventricle; 7n, facial nerve; 7, motor nucleus of the seventh nerve; 10, motor nucleus of the vagus nerve; 12, motor nucleus of the hypoglossal nerve; Amb, nucleus ambiguus; Cb, cerebellum; Ce, central nucleus of the amygdala; CPu, caudate/putamen; Cu, cuneate nucleus; DTg, dorsal tegmental nucleus; fr, fasciculus retroflexus; Gr, gracile nucleus; IC, inferior colliculus; IRt, intermediate reticular area (of medulla); LDTg, laterodorsal tegmental nucleus; LPB, lateral parabrachial nucleus; MHbD, MHbV, medial habenula; dorsal and ventral part;; RVLM, rostroventrolateral medulla; Thal, thalamus; Ve, vestibular area; VPL, ventral posterolateral thalamic nucleus. Scale: a,e, 500μm; d,g, 200μm; i, 100μm; j, 1mm.

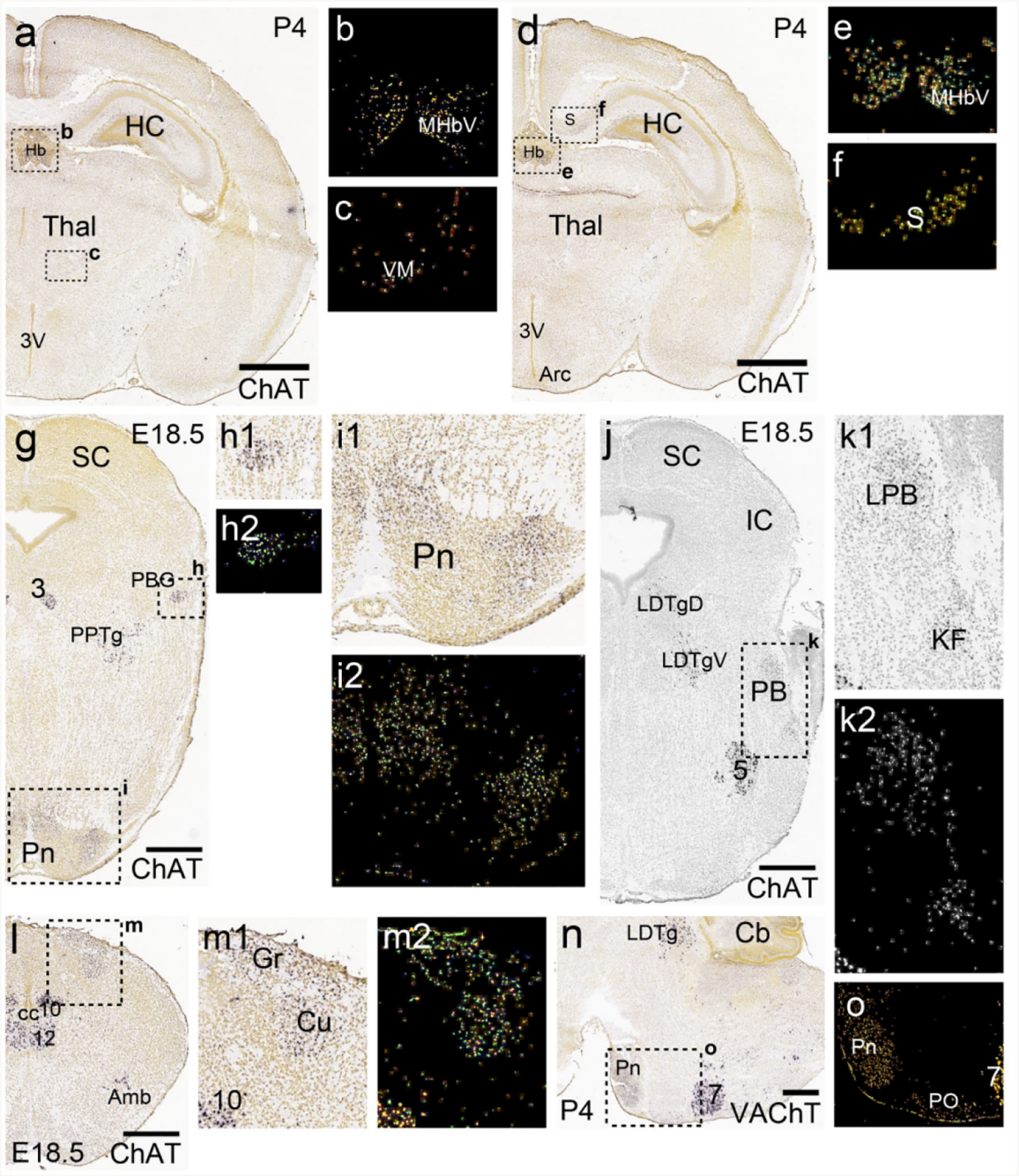

Figure 7. Late embryonic and early postnatal expression of ChAT mRNA in brain areas not known to be cholinergic.

ISH data are taken from the Allen Developing Mouse Brain Atlas. Sections are coronal except as noted. Developmental stages are selected based on the earliest available stages that show clear, robust expression of the specific mRNA. Insets show detail of hybridization signal and/or the corresponding “heat map” of expression data (Thompson et al., 2014). **(a–c)** Section at the level of the central thalamus and epithalamus at P4, corresponding to approximately bregma −1.7 in the adult mouse. (b) Heat map of expression in habenula. (c) Heat map of expression in the ventromedial thalamus. **(d–f)** Slightly more caudal view

showing expression in the subiculum. (e) Heat map of expression in habenula. (f) Heat map of expression in subiculum. **(g–i)** Midbrain and rostral pons at E18.5. ChAT expression is noted in the developing PBG (h) and pontine gray (i), as well as the known cholinergic area PPTg. **(j,k)** Midbrain and caudal pons at E18.5. ChAT is expressed in the parabrachial complex, probably representing the developing LPB and KF subnuclei, as well as the known cholinergic area LDTg. **(l,m)** Developing medulla at E18.5. ChAT is expressed in the cuneate and gracile nuclei, as well as the nuclei associated with hindbrain motor systems. **(n,o)** Sagittal section of the brainstem at P4, showing ISH signal for VAChT. Legend: 3V, third ventricle; 5, motor nucleus of the trigeminal nerve; 7, facial nucleus; 10, motor nucleus of the vagus nerve; 12, motor nucleus of the hypoglossal nerve; Amb, nucleus ambiguus; Arc, arcuate nucleus of hypothalamus; Cb, cerebellum; cc, central canal; Cu, cuneate nucleus; Gr, gracile nucleus; Hb, habenula; HC, hippocampus; IC, inferior colliculus; KF, Kölliker-Fuse nucleus; LPB, lateral parabrachial nucleus; LDTg, laterodorsal tegmental nucleus (D, dorsal, V, ventral part); MHbV, medial habenula, ventral part; PB, parabrachial nucleus; PBG, parabigeminal nucleus; Pn, pontine nucleus; PO, periolivary nucleus; PPTg, pedunculopontine tegmental nucleus; S, subiculum; SC, superior colliculus; Thal, thalamus; VM, ventromedial nucleus (of thalamus). Scale: a,d, 1mm; g,j,l,n, 500μm.

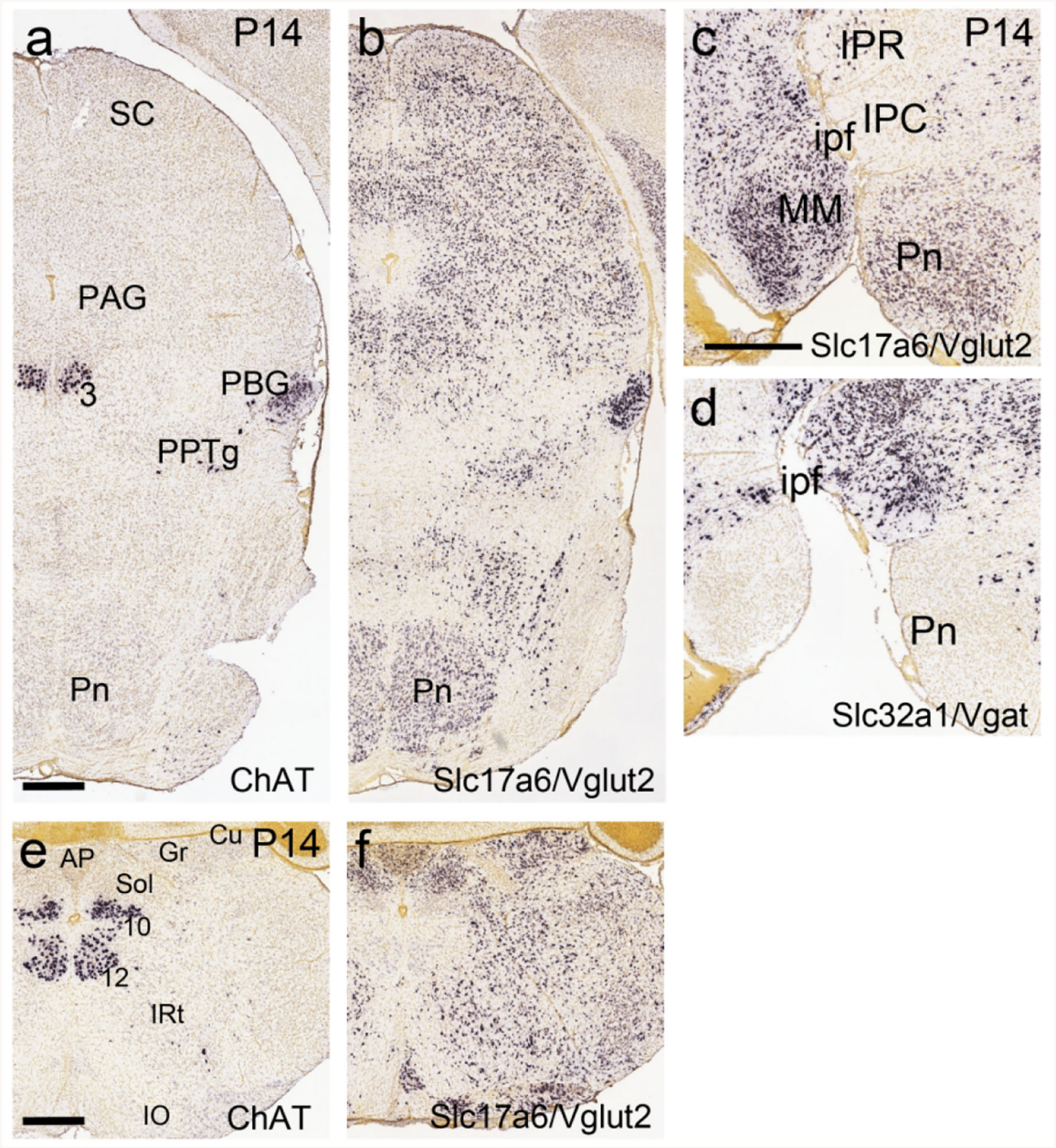

Figure 8. Extinction of ChAT expression, and expression of Slc17a6 (VGluT2), in the pontine and cuneate/gracile nuclei at postnatal day 14.

Data from the Allen Developing Mouse Brain Atlas. **(a,b)** Coronal section of the midbrain and pons. (a) ChAT mRNA is no longer detectable in the pontine nucleus at this stage. ChAT expression is still observed in PBG and oculomotor nucleus. (b) The pontine region is populated by glutamatergic neurons expressing VGluT2. PBG neurons appear to express VGluT2 as well as ChAT. **(c,d)** Sagittal sections of the pontine region, near the midline, hybridized for VGluT2 and Vgat mRNA. In (c), glutamatergic neurons expressing VGluT2 populate the pontine nucleus. In (d), few GABAergic neurons expressing Vgat are seen in the pontine nucleus, but are abundant in the adjacent IPR and IPC. **(e,f)** Coronal sections of the medulla hybridized for ChAT and VGluT2 mRNA. (e) ChAT mRNA is no longer

detectable in the cuneate and gracile nuclei at this stage. (f) The cuneate and gracile nuclei are populated predominantly with glutamatergic neurons expressing VGluT2. Legend: 3, oculomotor nucleus; 10, motor nucleus of the vagus nerve; 12, motor nucleus of the hypoglossal nerve; AP, area postrema; Cu, cuneate nucleus; Gr, gracile nucleus; IO, inferior olive; ipf, interpeduncular fossa; IPR, interpeduncular nucleus, rostral part; IPC, interpeduncular nucleus, caudal part; IRt, intermediate reticular area (of medulla); MM, medial mammillary nucleus; PAG, periaqueductal gray; PBG, parabigeminal nucleus; Pn, pontine nucleus; PPTg, pedunculopontine tegmental nucleus; SC, superior colliculus; Sol, nucleus of the solitary tract. Scale a–b,c–d,e–f: 500μm.

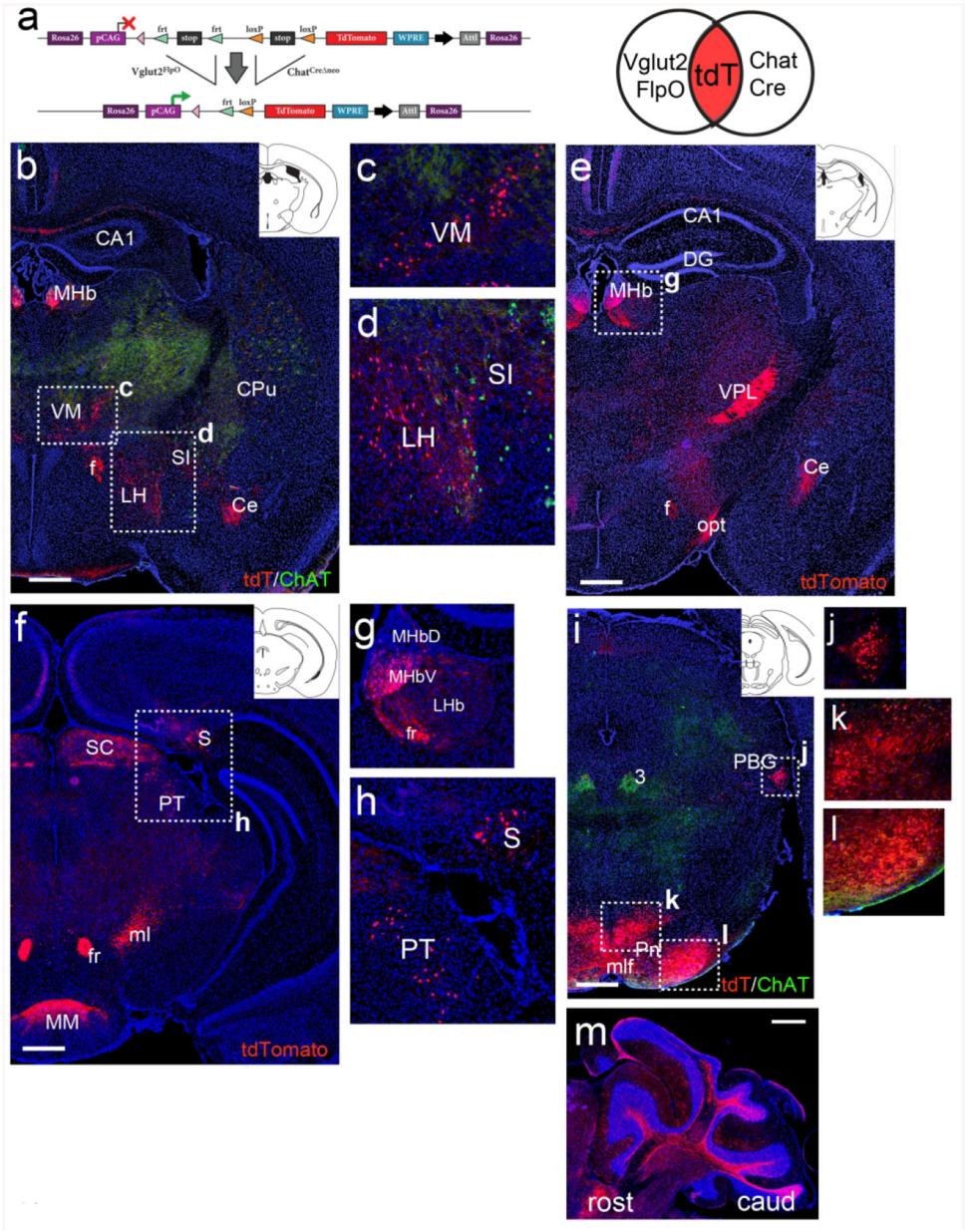

Figure 9. Dual recombinase fate-mapping of ChAT/VGluT2 co-expressing neurons in telencephalic, diencephalic, and mesopontine regions.

Coronal sections of adult Chat-Vglut2^{tdT} mice are shown except as noted. **(a)** Transgenic strategy for dual-recombinase labeling of neurons that co-express or sequentially express VGlut2^{FlpO} and Chat^{Cre}. Elements are not drawn to scale. Venn diagram illustrates that there is no expression of the tdT marker with Vglut2^{FlpO} or Chat^{Cre} alone, and that both recombinases must be or have been expressed to activate tdT expression. **(b–d)** Rostral thalamus and striatum (atlas level bregma −0.9, inset). Neurons in the MHb, VM and LH express tdT. Cholinergic neurons in the striatum (CPu, SI) express ChAT protein, but not tdT. Labeled fibers are evident in the amygdala. **(e–h)** Caudal thalamus and hypothalamus (bregma −1.6 and −2.9, insets). Neurons in the medial habenula, subiculum and a sparse

population in the pretectum express tdT. Fibers in opt and SC originate in the retina. Fibers in VPL originate in the cuneate/gracile nuclei. Fibers in MM originate in the subiculum. **(i–l)** Expression of tdTomato in the mesopontine area (bregma −4.2, inset). Neurons in PBG and in two areas of the pontine gray express tdTomato. **(m)** Sagittal section showing tdT expression in mossy fibers in the cerebellum, originating in the pontine nucleus. Legend: 3, oculomotor nucleus; CA1, CA1 region of hippocampus; Ce, central amygdala; CPu, caudate/putamen; DG, dentate gyrus; f, fornix; fr, fasciculus retroflexus; LH, lateral hypothalamus; LHb, lateral habenula; ml, medial lemniscus; mlf, medial longitudinal fasciculus; MHb, medial habenula (V, ventral, D, dorsal subnucleus); MM, medial mammillary nucleus; opt, optic tract; PBG, parabigeminal nucleus; Pn, pontine nucleus; PT, pretectum; S, subiculum; SC, superior colliculus; SI, substantia innominata; VM, ventromedial nucleus of thalamus; VPL, ventral posterolateral nucleus of thalamus. Scale: b,e,f,i,m, 500μm.

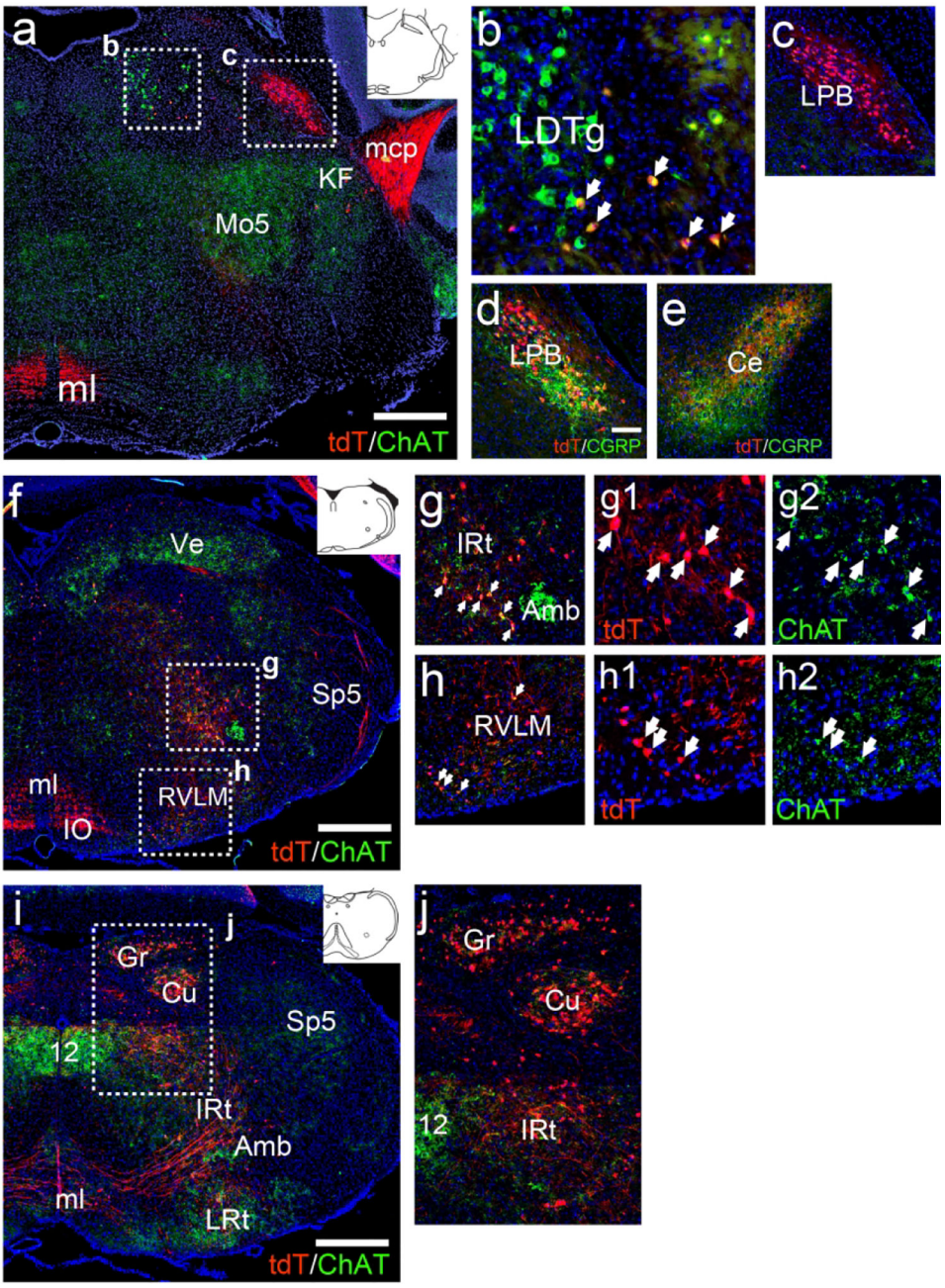

Figure 10. Dual recombinase fate-mapping of ChAT/VGluT2 co-expressing neurons in the brainstem.

Coronal sections of adult Chat-Vglut2^{tdT} mice are shown. **(a–c)** Expression of tdT and ChAT protein in the mesopontine area (atlas level bregma −5.1, inset). Cholinergic brainstem motor neurons, such as those in 5, express ChAT protein but not tdTomato. Pontocerebellar fibers are labeled with tdTomato in the mcp. (b) A small population of cholinergic neurons in the ventrolateral LDTg co-express tdTomato. (c) LPB neurons express tdTomato but no longer express detectable levels of ChAT protein. **(d)** In the LPB CGRP immunoreactivity co-localizes with tdTomato. **(e)** CGRP and tdTomato co-localize in

LPB afferents terminating in the amygdala. **(f–h)** Expression of tdTomato and ChAT protein in the rostral medulla (bregma −6.6, inset). Ascending fibers from the cuneate/gracile nuclei are labeled with tdTomato in ml. (g,h) Detail of IRt and RVLM shows low levels of ChAT protein persist in tdTomato-expressing neurons in these areas. **(i–j)** Expression of tdTomato and ChAT protein in the caudal medulla (bregma −7.6, inset). (j) Detail of Cu/Gr, and caudal IRt. A few neurons in these area express low levels ChAT protein. Legend: 12, motor nucleus of the hypoglossal nerve; Amb, nucleus ambiguus; Ce, amygdala, central nucleus; Cu, cuneate nucleus; Gr, gracile nucleus; IO, inferior olive; IRt, intermediate reticular nucleus (of medulla); KF, Kölliker-Fuse nucleus; LDTg, laterodorsal tegmental nucleus; LPB, lateral parabrachial nucleus; LRt, lateral reticular nucleus (of medulla); mcp, middle cerebellar peduncle; ml, medial lemniscus; Mo5, motor nucleus of trigeminal nerve; RVLM, rostroventrolateral medulla; Sp5, trigeminal nucleus, spinal part; Ve, vestibular nuclei. All sections are counterstained with DAPI (blue). Scale: a,f,i, 500μm; d–e, 100μm.

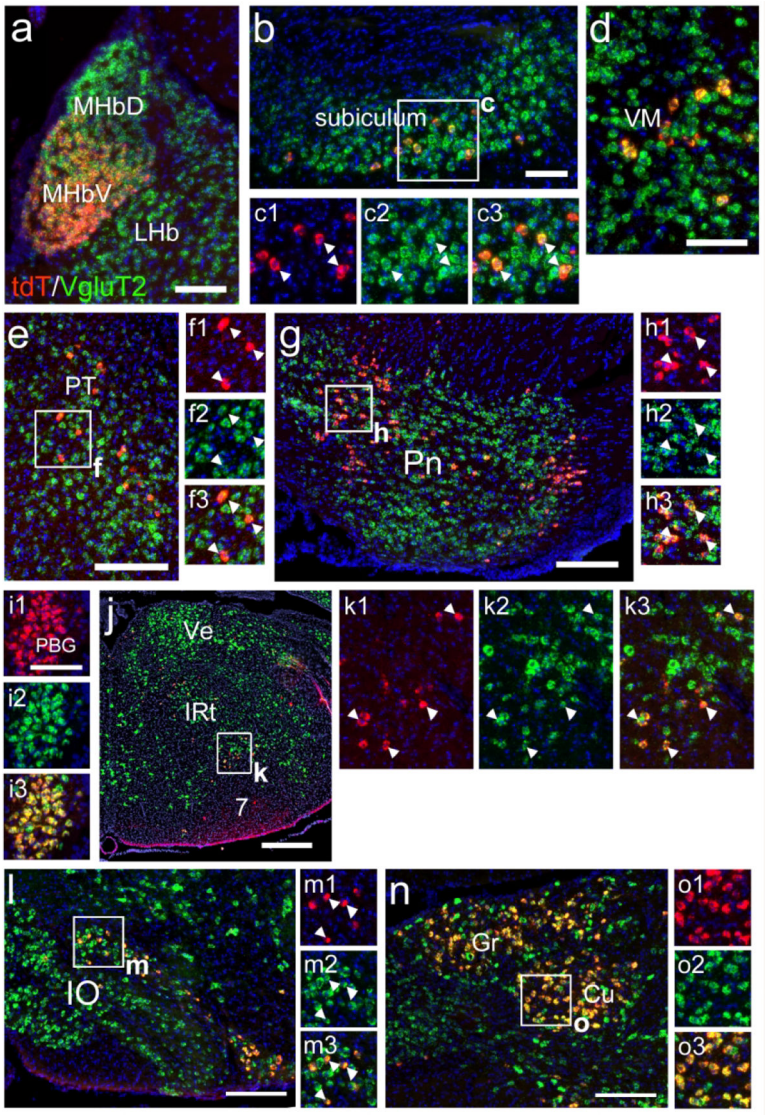

Figure 11. Expression of Vglut2 mRNA in Chat-Vglut2^{tdT} expressing neurons.

Fluorescence *in situ* hybridization was performed for tdTomato mRNA encoded by the Chat-Vglut2^{tdT} transgene and endogenous VgluT2 mRNA. **(a)** Expression in the habenula, at a rostrocaudal level similar to that shown in Figure 8b. **(b,c)** Expression in the subiculum. **(d)** Expression in VM, similar to 8c. **(e,f)** Expression in the pretectum, similar to 8h. **(g,h)** Expression in the pontine nucleus, similar to 8i,k,l. **(i)** Expression in PBG, similar to 8j. **(j,k)** Expression in the medulla, at a level slightly rostral to that shown in 9f. Inset (k) shows area corresponding to the post-inspiratory complex. **(l,m)** Expression in the IO, similar to 3g. **(n,o)** Expression in Cu/Gr, similar to 9j. Legend: 7, motor nucleus of the facial nerve; Cu, cuneate nucleus; Gr, gracile nucleus; IO, inferior olive; IRt, intermediate reticular nucleus (of medulla); LHb, lateral habenula; MHb, medial habenula (V, ventral, D, dorsal subnucleus); PBG, parabigeminal nucleus; Pn, pontine nucleus; PT, pretectum; Ve, vestibular area; VM, ventromedial nucleus of thalamus. All sections are counterstained with DAPI (blue). Scale: a,b,d, i, 100μm; e,g,l,n, 200μm; j, 500μm.

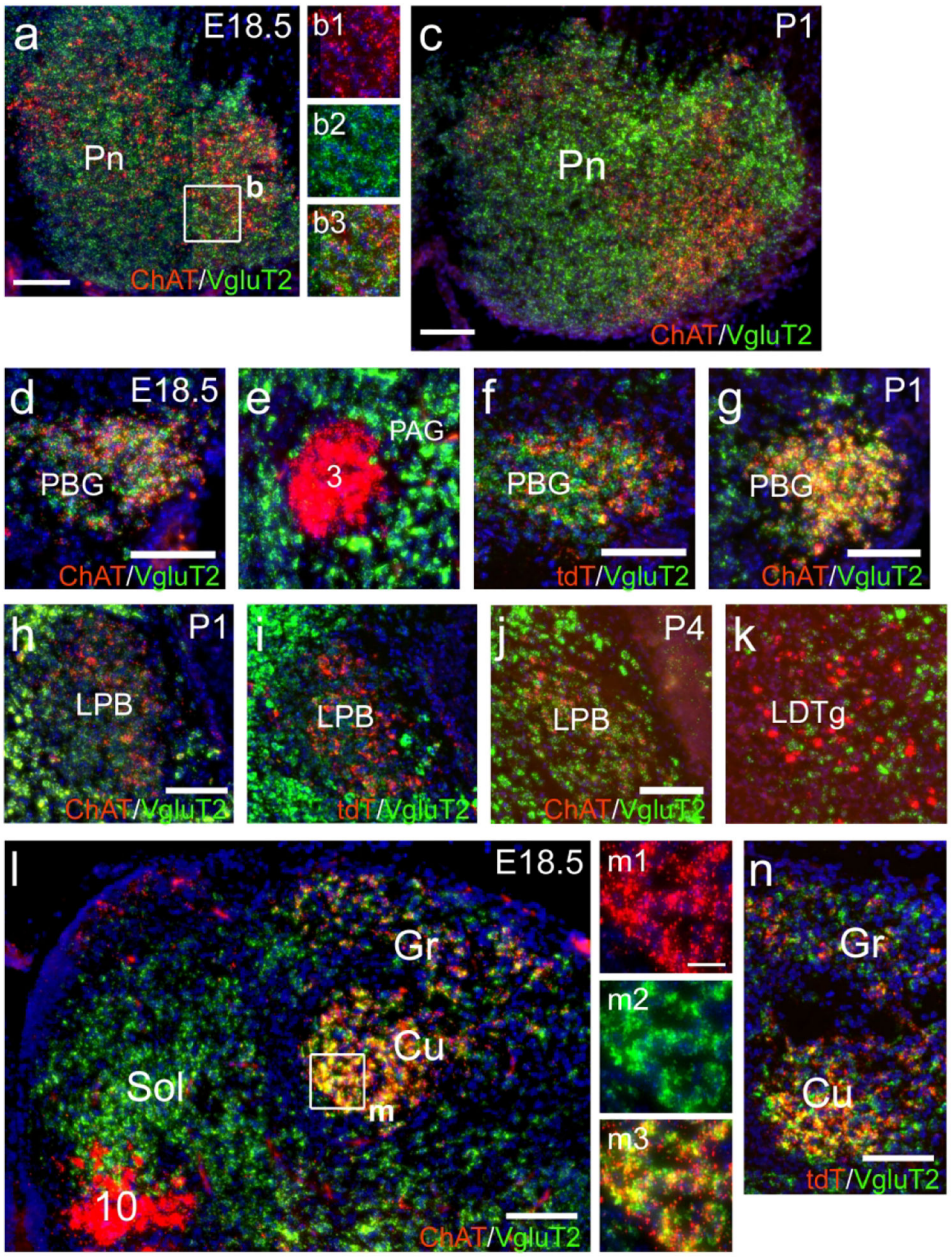

Figure 12. Developmental timing of ChAT/VgluT2 co-expression in the brainstem.

Fluorescence *in situ* hybridization was used to examine the expression of ChAT mRNA or tdTomato mRNA together with VgluT2 mRNA in the developing mouse brainstem near the time of first detection of ChAT expression. **(a,b)** Expression of ChAT and VgluT2 in the condensing pontine nucleus at E18.5. **(c)** Expression in the pontine nucleus at P1. **(d–f)** Expression in tegmentum at E18.5. (d) Shows co-expression of ChAT and VgluT2 in the PBG, while (e) shows discrete expression in the oculomotor nucleus and surrounding PAG, from the same section and image as (d). (f) tdT and VgluT2 in the PBG. **(g)** Expression of ChAT and VgluT2 in the PBG at P1. **(h,i)** Expression in the LPB at E18.5. (h) Expression of ChAT and VgluT2. (I) Expression of tdT and Vglut2. **(j,k)** Expression of ChAT and VgluT2

in the tegmentum at P4. (j) Shows co-expression of the markers in LPB, while (k) shows discrete expression in the LDTg, from the same section and image as (d). **(l–n)** Expression in the dorsal medulla at E18.5. (l) Co-expression of Chat and VgluT2 is seen in the gracile and cuneate nuclei, while discrete expression is seen in Sol and 10. Legend: 3, oculomotor nucleus; 10, motor nucleus of the vagal nerve; Cu, cuneate nucleus; Gr, gracile nucleus; LBP, lateral parabrachial nucleus; LDTg, laterodorsal tegmental nucleus; PAG, periaqueductal gray; PBG; Pn, pontine nucleus; Sol, solitary nucleus. Scale: a-l, n, 100μm; m, 20μm.

Cholinergic neurons not expressing Vglut2

Cerebral cortex, non-pyramidal neurons[1]
Septum/diagonal band: MS,LS, DB
Striatum: CPu,VP[2]
Basal forebrain: SI, NBM
Arcuate nucleus
Mesopontine areas: PPTg, LDTg[3]
Brainstem motor neurons: 3,4,6,5,7,10,12
Brainstem autonomic neurons

ChAT expression in neurons with transient or persistent co-expression of cholinergic markers and Vglut2

Stage:	E16	E18	P1	P4	P7	P60
Hippocampus: subiculum	−	−	•	●	•	Ø
Thalamus: ventromedial	−	−	•	●	•	Ø
Hypothalamus: rostrolateral	−	•	•	●	•	Ø
Habenula: medial, ventral	−	−	●	●	●	●
Mesopontine: pretectum	−	−	−	●	•	Ø
Mesopontine: PBG	●	●	●	•	•	•
Mesopontine: pontine gray	−	−	●	●	●	Ø
Mesopontine: LBP/CGRP	−	●	●	●	•	Ø
Mesopontine: LBP/KF	−	●	●	●	•	•
Medulla: PO, RVLM	●	●	●	●	●	●
Medulla: IRt “PiCo”	−	●	●	●	●	●
Medulla: inferior olive	−	●	•	•	Ø	Ø
Medulla: gracile/cuneate[4]	●	●	●	●	●	(•)

Figure 13. Summary of co-expression patterns of ChAT and VGluT2.

Top: List of Chat^{tdT}-expressing neurons in known cholinergic populations that did not show reporter activation with Vglut2^{Flp}. **Bottom:** Developmental time course of ChAT protein expression in Chat^{tdT} neurons in brain regions that express Chat-Vglut2^{tdT}. Filled circles indicate the intensity of ChAT immunostaining in neurons expressing Chat^{tdT} in the listed structure. A minus (−) sign indicates that Chat^{tdT} was not yet detectable at the designated stage. A null sign (Ø) indicates that ChAT immunoreactivity was below the threshold of detection in Chat^{tdT} expressing neurons. Quantitation is based on visual comparison of the signal intensity in the transiently cholinergic neurons to the neurons at with the highest expression of ChAT on the same slide. The most strongly ChAT immunopositive reference neurons include striatal cholinergic neurons (forebrain), LDTg cholinergic neurons

(mesopontine area), and motor neurons associated with the cranial nerves 3, 5, 7 and 10/12. Legend: (1) In the telencephalic domain of VGluT1 expression, VGluT2 expression is not expected; (2) VGluT3 is expressed in the striatum; (3) Very sparse Chat-Vglut2^{tdT} expression is observed in PPTg and LDTg; (4) Trace expression of ChAT immunoreactivity is observed in the adult gracile/cuneate, not clearly associated with cell somata.